U.S.NRC
United States Nuclear Regulatory Commission
Protecting People and the Environment

RIL 2023-04

Paleoliquefaction Studies of the Central Virginia Seismic Zone

Date Published: April 2023

Prepared by:

M. P. Tuttle, M. Tuttle & Associates
P.O. Box 345, Georgetown, ME 04548

K. Dyer-Williams, VanLeen Associates
P.O. Box 156, Columbia, MD 21045

K. Tucker, PangaeaGIS
2065 Leichester Lane, Memphis, TN 38134

Rasool Anooshehpoor, NRC Program Manager

Research Information Letter
Office of Nuclear Regulatory Research

DISCLAIMER

Legally binding regulatory requirements are stated only in laws, NRC regulations, licenses, including technical specifications, or orders; not in Research Information Letters (RILs). A RIL is not regulatory guidance, although NRC's regulatory offices may consider the information in a RIL to determine whether any regulatory actions are warranted. This report was prepared as an account of work sponsored by an agency of the United States Government. Neither the United States Government nor any agency thereof, or any of their employees, makes any warranty, expressed or implied, or assumes any legal liability of responsibility for any third party's use, or the results of such use, or any information, apparatus, product or process disclosed in this report, or represents that its use by such third party would not infringe privately owned rights.

ABSTRACT

Sand dikes and injected krotovinas along the Appomattox River southwest of Richmond are likely to be earthquake-induced liquefaction features that formed during probably a historical earthquake and a paleoearthquake between 3450-2450 yr before present (B.P.). This finding is consistent with previous findings of two generations of liquefaction features along other rivers in the Central Virginia seismic zone (CVSZ). Pseudonodules, diapirs, flames and a sand dike along the Rapidan River west of Fredericksburg might be earthquake-induced liquefaction features that formed during either a pre-instrumental earthquake or a previously unrecognized paleoearthquake between 1830-60 yr B.P. The sand dikes and other soft-sediment deformation structures were found during surveys of ~106 km of the Appomattox, Mattaponi, Rapidan, Rappahannock, and Potomac Rivers as well as estuaries of the Popes, Rosier, and Upper Machodoc Creeks as part of an effort to better understand the earthquake potential of the CVSZ following the 2011, moment magnitude, **M**, 5.7 ± 0.1 Mineral, Virginia, earthquake. The surveys extend the area searched for liquefaction features beyond previously found features and towards the margins of the CVSZ. The Appomattox features extend the area of historical and prehistorical liquefaction towards the southern margin of the seismic zone, and dating of the older features helps to better constrain the age of the paleoearthquake that appears to have induced liquefaction in susceptible alluvium across the zone. The Rapidan features might extend the area of historical or prehistorical liquefaction towards the north. No liquefaction features were found along the other rivers surveyed. The absence of features along the Mattaponi River near Beulahville suggests that ground motion was not strong enough to induce liquefaction in this area during historical earthquakes or the paleoearthquake ~3 ka ± 500 yr. For the other rivers and estuaries, however, the sedimentary conditions were not conducive to the formation of liquefaction features and/or the exposure of sediment was not adequate to find liquefaction features, if they were present. The relation between earthquake magnitude and liquefaction distance as well as liquefaction potential analysis were used to evaluate scenario earthquakes and possible locations and magnitudes of earthquakes that induced liquefaction in the CVSZ. Although other interpretations are possible, the results suggest that historical liquefaction features along the Appomattox, James, and Pamunkey Rivers formed as result of three **M** 5.0-5.5 earthquakes, likely the 1758, 1774, and 1875 events, located close to the three groups of features and that prehistorical liquefaction features along the Appomattox, Mattaponi, Pamunkey, Rivanna, and South Anna Rivers formed during one **M** 6.5-6.75 paleoearthquake near Holly Grove or farther east between the Appomattox and Mattaponi Rivers. This study contributes to knowledge of the record of earthquake-induced liquefaction in and the earthquake potential of the CVSZ, though uncertainties remain regarding the origin and age of some of the features, as well as the extent of liquefaction especially in the southern CVSZ. These uncertainties could be further reduced and interpretations tested, with additional survey for, study and dating of, earthquake-induced liquefaction features.

FOREWORD

The U.S. Nuclear Regulatory Commission (NRC) requires an evaluation to determine the Safe Shutdown Earthquake (SSE) ground motion for a nuclear power plant site as specified in 10 CFR Part 100. A performance-based approach to define site-specific earthquake ground motion is one component in the development and evaluation of the SSE. Regulatory Guide 1.208 provides guidance on this performance-based approach which implements a probabilistic seismic hazard analysis. The probabilistic seismic hazard analysis is dependent on the characterization of seismic (earthquake) sources, with the key parameters in characterizing seismic sources being their location, timing, and size. The historical record of measured earthquakes is limited; therefore, the study of prehistoric earthquakes is extremely valuable in characterizing seismic sources. The study of prehistoric liquefaction features, paleoliquefaction, is one method used to characterize seismic sources.

Regulatory Guide 1.208, A Performance-Based Approach to Define the Site-Specific Earthquake Ground Motion, and the Standard Review Plan for the Review of Safety Analysis Reports for Nuclear Power Plants: LWR Edition (NUREG-0800), Section 2.5.1, provides guidance to license applicants and NRC staff, respectively, on the review of seismic sources. This document provides valuable information about the approximate timing, locations, and magnitudes of past earthquakes in the Central Virginia Seismic Zone (CVSZ) and surrounding region, key parameters for the assessment of earthquake hazard in the Mid-Atlantic region and Greater Washington D.C. area. The document also serves as an example of how to conduct a paleoliquefaction study and to evaluate data and their uncertainties for seismic source characterization.

TABLE OF CONTENTS

LIST OF FIGURES

LIST OF TABLES

ACKNOWLEDGMENTS

This research project is sponsored by the U.S. NRC under contract 31310019C0028. The views and conclusions contained in the document are those of the authors and should not be interpreted as necessarily representing the official policies of the U.S. Government. Many thanks to Rasool Anooshehpoor of the NRC who provided valuable guidance and support throughout the contract. Carlos Velez and Laurel Bauer provided valuable assistance during field work. Carl Benson and Ramesh Neupane of the Virginia Department of Transportation provided access to geotechnical data for the project. Radiocarbon and optically-stimulated luminescence dating were performed by Beta Analytic, Inc. and Geoluminescence Dating Research Lab at Baylor University, respectively. Many thanks to the National Park Service for permission to conduct research at the George Washington Birthplace National Monument and to property owners who gave access to the rivers. Martin Chapman, Mark Carter, Jeff Munsey, and Thomas Pratt provided background information and helpful suggestions during this project. Rasool Anooshehpoor, Thomas Weaver, and Laurel Bauer reviewed this report and provided helpful comments and suggestions.

1 INTRODUCTION

On August 23, 2011, a moment magnitude, **M** 5.7 ± 0.1 earthquake occurred near Mineral, Virginia, about 60 km northwest of Richmond and 130 km southwest of Washington, D.C. (Figure 1-1; Horton et al., 2015). The earthquake resulted from a complex rupture including three subevents that define a small source area 6–8 km below the surface (Chapman, 2013). Peak ground acceleration (PGA) of 0.27 g, measured 23 km northeast of the epicenter at the North Anna nuclear power plant, was greater than the 2% probability of exceedance for hard rock on the seismic hazard maps of the region at the time (Petersen et al., 2008). The Mineral earthquake induced liquefaction in alluvial deposits along the South Anna River (Green et al., 2015) in an area that likely experienced especially high ground motion based on modeling of PGA (Chapman, 2015). The earthquake also caused damage to residences, buildings, schools, and earthen dams in the epicentral area (Green et al., 2015) and to bridges, prominent buildings, and monuments in Washington, D.C. (Horton et al., 2015). Crowd-sourced intensity data collected by the U.S. Geological Survey (USGS) suggested amplification at sediment sites around the Chesapeake Bay, in the Washington, D.C., and other coastal cities, as well as source directivity and more efficient wave propagation along the northeast-southwest-striking structural grain (Hough, 2012). A subsequent site response study found significant amplification of ground motions in Washington, D.C., where Atlantic Coastal Plain and other unconsolidated sediment overlie crystalline bedrock (Pratt et al., 2017).

The 2011 Mineral earthquake occurred in the Central Virginia seismic zone (CVSZ), an area of diffuse seismicity with most earthquakes occurring within ~60 km of the James River and between Richmond and Charlottesville, VA (Figure 1-1; Chapman, 2013 and 2015). According to the catalog of earthquakes developed by the USGS, the 1758 **M** 4.95 ± 0.37 event near Ruther Glen, the 1774 **M** 4.43 ± 0.5 event near Petersburg, and the 1875 **M** 4.77 ± 0.35 event northwest of Goochland were the three largest pre-instrumental earthquakes to have occurred in the CVSZ prior to 2011 (Mueller et al., 2018; Rukstales and Petersen, 2019). According to the earthquake catalog developed for the Central and Eastern U.S. Seismic Source Characterization Project, the estimated horizontal location uncertainty for these pre-instrumental earthquakes ranges from 34–50 km, and the 1875 earthquake may have been ~60 km southwest of the USGS location (EPRI et al., 2012; Figure A-1 shows horizontal or epicentral error ellipses for the 1758, 1774, and 1875 earthquakes). In an unpublished evaluation of felt reports, the 1774 earthquake is thought to have been at least as large as a **M** 5.0 and may have been located in or near Amelia County northwest of Petersburg (Jeff Munsey, oral communication, Jan. 2021).

The 2011 **M** 5.7 mainshock is the largest known earthquake to have occurred in the CVSZ and raised concerns about the earthquake potential of this seismic zone. The estimated return period for $m_{blg} \geq 6.3$ earthquakes, like the 2011 Mineral event, is ~750 yr, with a 95% confidence interval of 385–1471 yr (Chapman, 2015). As suggested for other seismically active areas along the Atlantic passive margin, the CVSZ may include events of a prolonged aftershock sequence of a large prehistoric earthquake (Ebel et al., 2000; Wolin et al., 2012). If so, the short-term historical seismicity might underrepresent the long-term earthquake potential of the seismic zone. The 2011 **M** 5.7 Mineral earthquake, like the 1988 **M** 5.9 Saguenay, Quebec, and 2011 **M** 6.3 Christchurch, New Zealand, events, was not associated with surface rupture but did induce liquefaction (Figure 1-1 and Figure 1-2; Tuttle et al., 1990; Green et al., 2015; Tuttle et al., 2017). Paleoearthquakes similar to these events would be missed with the fault-trenching approach in paleoseismology but could be recognized with the paleoliquefaction approach (e.g., Obermeier, 1996; Tuttle, 2001; Green et al., 2005; Tuttle et al., 2019a).

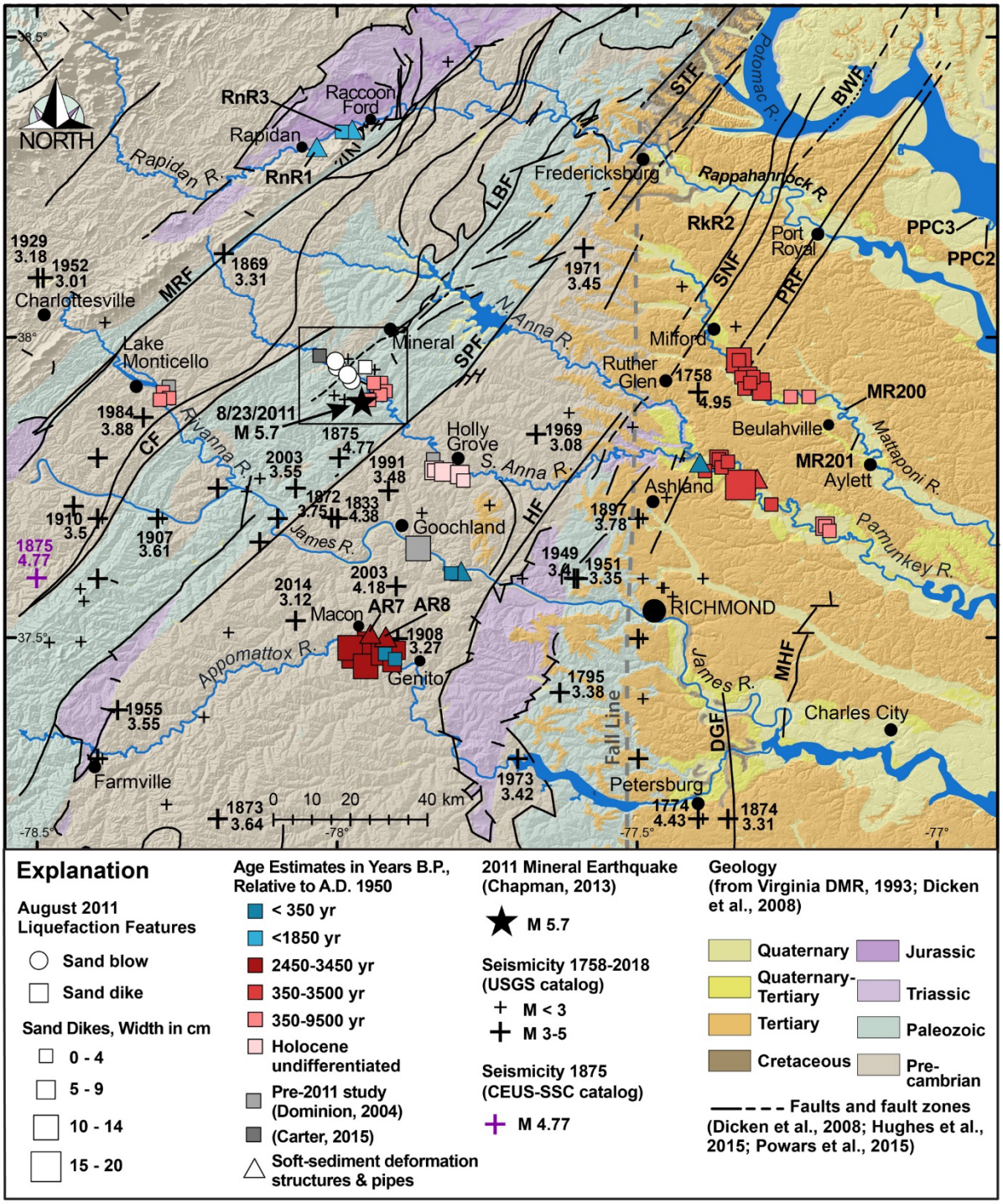

Figure 1-1: **Map of the CVSZ showing 2011 Mineral earthquake (black star), sand blows that formed in 2011 epicentral area (white circles) and liquefaction features found during pre- and post-2011 studies. Liquefaction features on Appomattox and Rapidan Rivers were found during this study. Epicentral area of 2011 Mineral earthquake shown in Figure 1-2 indicated by black square. Fault zones: MRF=Mountain Run; STF= Stafford; HF=Hylas; SNFZ=Skinkers Neck; PRFZ= Port Royal; MF=Malvern Hill.**

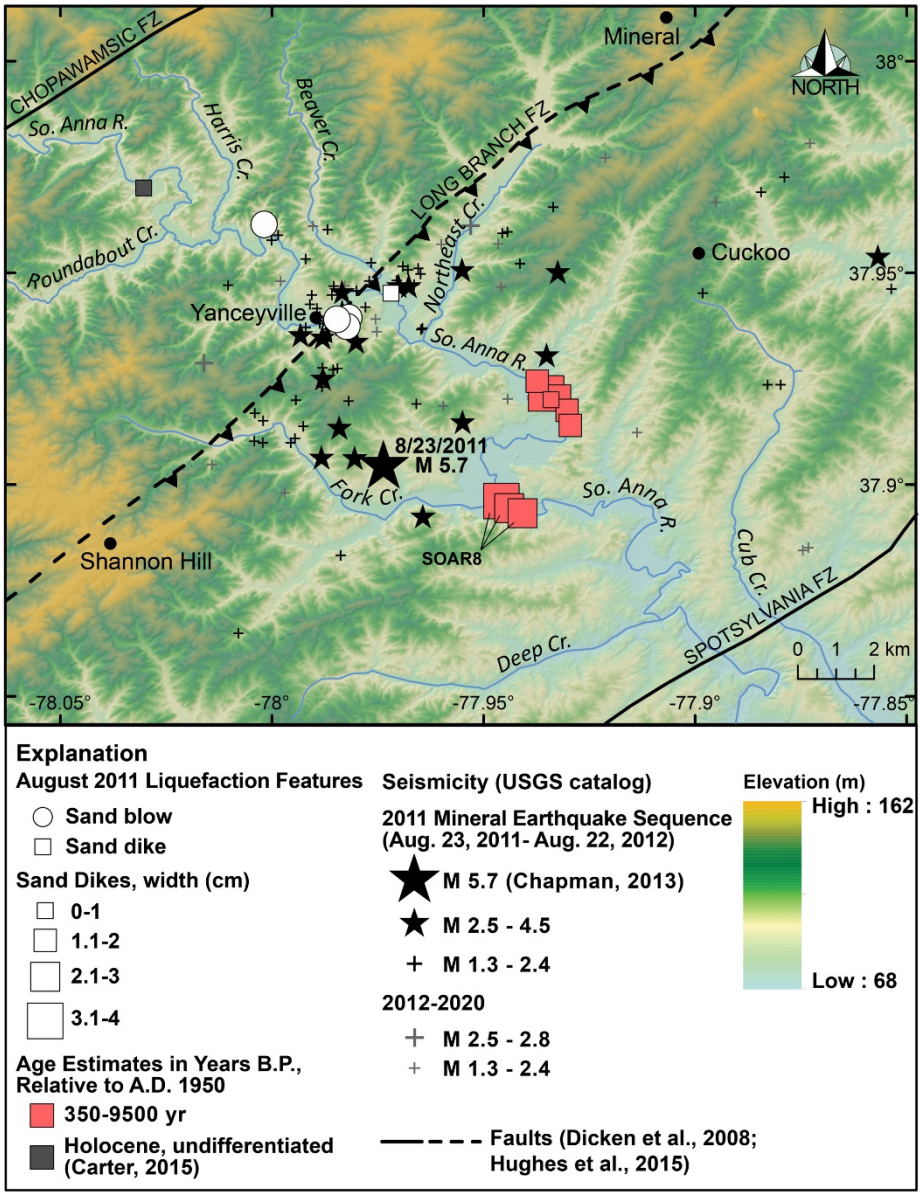

Figure 1-2: Epicentral area of 2011, M 5.7, Mineral earthquake, aftershocks, and subsequent earthquakes, liquefaction features that formed during the 2011 mainshock, and older liquefaction features found during river survey. Area of figure indicated on Figure 1-1.

Paleoliquefaction studies have helped to assess the earthquake potential of other seismic zones in Central and Eastern North America (see Tuttle and Hartleb, 2012 for a review of regional studies) and are proving useful in the CVSZ. As described in more detail in Section 2 below, paleoliquefaction studies conducted 10-15 years before the 2011 Mineral earthquake and during the 10 years following the event found evidence of strong ground shaking caused by moderate to large earthquakes during the Holocene (0.0117 million years ago, or Ma, to present; Cohen et al., 2022). This study builds on previous studies and extends the search for liquefaction features beyond recently found liquefaction features and towards the eastern, northeastern, northern, and southern margins of the CVSZ.

2 PREVIOUS PALEOLIQUEFACTION STUDIES

During a paleoliquefaction study conducted in the mid-1990s, several weathered sand dikes (1 to 10 cm wide) were found at one site each on the James, Rivanna, and South Anna Rivers (Figure 1-1; Obermeier and McNulty, 1998; Dominion, 2004). The paleoliquefaction features were attributed to at least one, and possibly three, moderate earthquakes during the Holocene. The apparent lack of widespread liquefaction features was interpreted as evidence that an earthquake of **M** > 7 had not occurred in the CVSZ during the past 10,000 years, though an earthquake in the **M** 6 to 7 range was not ruled out (Obermeier and McNulty, 1998; Dominion, 2004). A similar conclusion was reached by a review of liquefaction features at the three sites following the 2011 Mineral earthquake (Schindler et al., 2012).

During a post-event survey of the 2011 Mineral earthquake, four small sand blows were found in and adjacent to the South Anna River in the Yanceyville area, indicating that the moderate earthquake induced liquefaction in the epicentral area (Figure 1-1 and Figure 1-2—white circles; Green et al., 2015; Jeff Munsey, Tennessee Valley Authority, oral communication, Jan. 2021). Later in the fall of 2011 following several storms, including Hurricane Irene, reconnaissance was performed in the Yanceyville area and downstream for 24 km along the South Anna River. No additional sand blows were found on the South Anna River flood plain, but one small (1 cm wide) and unweathered sand dike that likely formed in 2011 was found in a cutbank exposure about 1 km northeast of Yanceyville (Figure 1-1 and Figure 1-2—white square; Tuttle et al., 2019b). Farther downstream, paleoliquefaction features, mostly bioturbated and weathered sand dikes, ranging in width from 1-5 cm, were found at eight sites along the river. It was suggested that the paleoearthquake(s) responsible for the features may have been larger, and/or located farther to the east, than the 2011 event (Tuttle et al., 2019b).

A subsequent paleoliquefaction study in 2015 involved surveys for paleoliquefaction features along (1) two segments of the South Anna River downstream from Yanceyville, (2) the Mattaponi and Pamunkey Rivers east of the Fall Line, where liquefiable sediments are more common than in the epicentral area of the Mineral earthquake; (3) the Rivanna River and Stigger Creek, where several sand dikes were found in the 1990s; and (4) the James River south of the Mineral earthquake (Figure 1-1 and Figure 2-1; Tuttle et al., 2021). During the surveys, forty-one sand dikes, sand sills, and soft-sediment deformation features were found at twenty-four sites. The liquefaction features were attributed to at least two episodes of earthquake-induced liquefaction prior to 2011 based on dating of host sediments and weathering characteristics of the features. Dating suggested that the younger generation of features formed during the past 350 years, and the older generation of features formed between 350 and 2800 years ago. There were no crosscutting relationships of the paleoliquefaction features or significant difference in their weathering characteristics to suggest multiple events, though this possibility could not be ruled out.

Evaluating scenario earthquakes that could account for the areal distribution of liquefaction features, it was found that the 1758, 1774, and/or 1875 earthquakes could have been responsible for the formation of the historical liquefaction features, if two of the events were of **M** 5–5.25 and located within 5–14 km of the sites on the James and Pamunkey Rivers, or if one of the events were of **M** 5.75 and located between the two rivers (Tuttle et al., 2021). For the prehistorical liquefaction features, three possible source areas for paleoearthquake(s) were considered, near Mineral, Holly Grove, and Ashland, though other events or combinations of events might explain the liquefaction features. It was found that one event of **M** 6.5 near Holly Grove or two events of **M** 6.0 and **M** 6.25 near Mineral and Ashland, respectively, could account for the regional

distribution of paleoliquefaction features, as could a **M** 6.25 near Holly Grove if Coastal Plain sediment sufficiently amplified ground motions along the Mattaponi River.

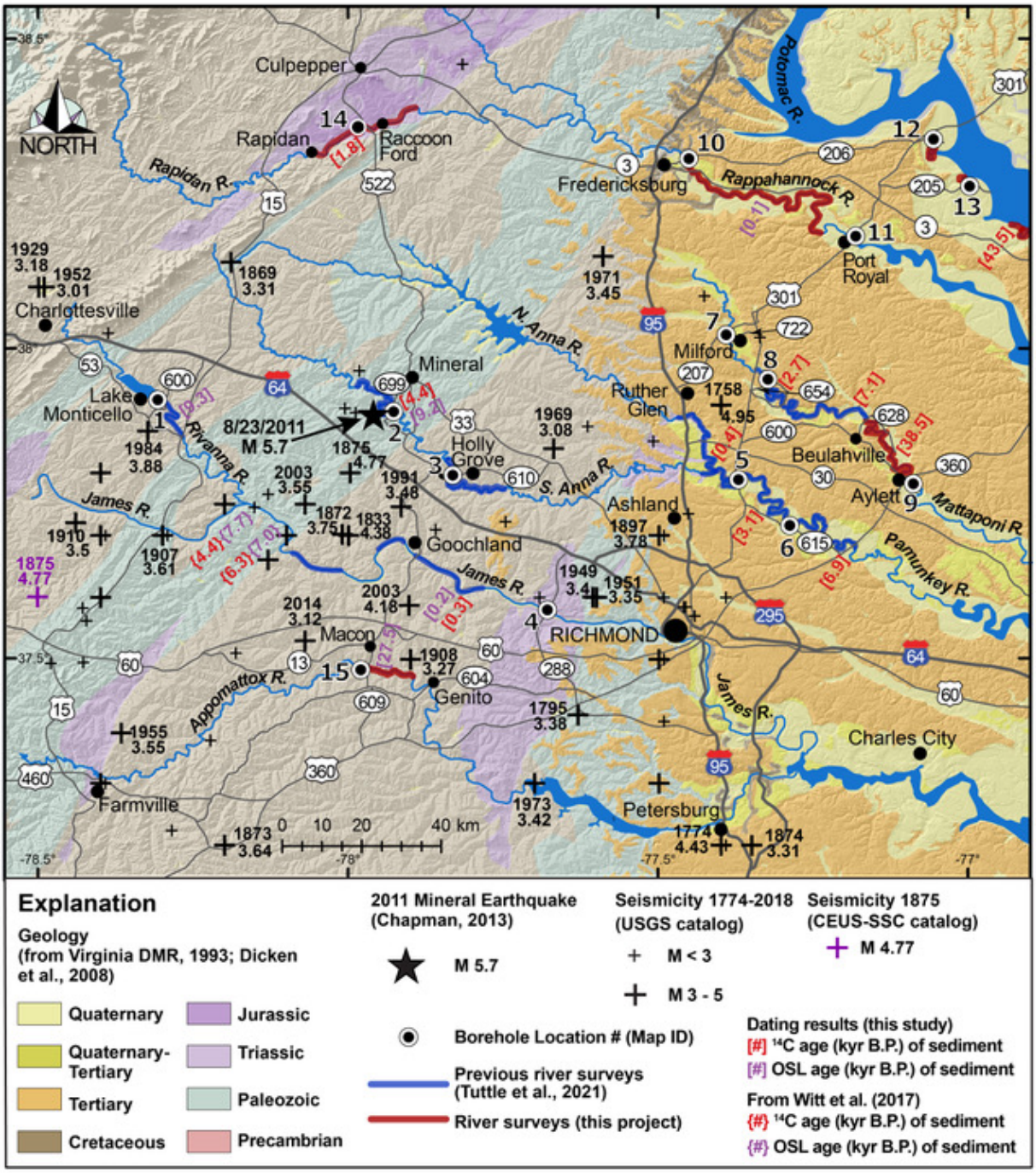

Figure 2-1: Map of CVSZ and surrounding region showing seismicity and location of 2011, M 5.7, Mineral earthquake, portions of rivers examined for earthquake-induced liquefaction during this study (thick red lines) and previous study (thick purple lines), radiocarbon (C14) and optically-stimulated luminescence (OSL) ages of exposed sediment, and locations of boreholes logs used in the evaluation of scenario earthquakes.

3 METHODOLOGY

This study employs best practices as described in the NUREG/CR-7238 (Tuttle et al., 2018) and review article in Geosciences (Tuttle et al., 2019a). Geological maps, geotechnical data, and satellite imagery were reviewed to identify river segments where conditions may be favorable for the formation and preservation of earthquake-induced liquefaction features and where exposure may be adequate to find features, if present (Table B-1, Table B-2, and Table B-3). On the basis of the review, river segments were inspected in the field to further assess sedimentary conditions and cutbank exposures and to locate access points and permissions. Following the field inspections, specific river segments were selected for surveys to be carried out when water levels were low and cutbanks exposed (Figure 2-1, thick red lines delineate river segments selected for river surveys).

During the surveys, sediment exposed in cutbanks was examined for the presence or absence of earthquake-induced liquefaction features. Identification of liquefaction features was based on diagnostic criteria developed from studies of liquefaction features that formed during modern and historical earthquakes (Tuttle et al., 2019a). Site locations were measured with a hand-held global positioning system and marked on topographic maps, site conditions recorded, and liquefaction features described in terms of sedimentary and weathering characteristics, size, orientation, and lateral and vertical continuity. Information about the study sites and liquefaction features are summarized in Table C-1 and locations, sizes, and estimated ages of liquefaction features are shown on Figure 1-1. Organic and sediment samples were collected along the rivers and results of radiocarbon (C14) and optically-stimulated luminescence (OSL) dating are provided in Table D-1 and Table D-2, respectively. Dating results are used to estimate the ages of sediment and liquefaction features found along the rivers. Information about liquefaction features, dating results, and age estimates were entered into a geodatabase and ArcGIS was used to generate project maps (Figure 1-1, Figure 1-2, and Figure 2-1).

For this study, newly found and dated liquefaction features were considered along with previously found liquefaction features to estimate the timing, locations, and magnitudes of earthquakes that led to their formation. Scenario earthquakes were evaluated to help constrain the locations and magnitudes of causative earthquakes using both the empirical relation between earthquake magnitude and epicentral distance to farthest liquefaction (e.g., Ambraseys, 1988; Castilla and Audemard, 2007) and the cyclic stress method for assessing liquefaction potential (e.g., Seed and Idriss, 1971 and 1982; Youd and Idriss, 2001; Cetin et al., 2004; Idriss and Boulanger, 2004; Green et al., 2005; Tuttle et al., 2019a). Magnitude estimates based on the cyclic stress method may be more realistic than those derived from the magnitude-distance relation, since liquefaction potential analysis uses local geotechnical data (i.e., blow counts related to soil density and liquefaction susceptibility) whereas the magnitude-distance relation is based on cases studies of liquefaction from around the world that occurred in especially susceptible sediment. Site amplification related to soil conditions is factored into liquefaction potential analysis but does not replace response analysis using site-specific velocity profiles.

The magnitude-distance relation and the results of the evaluation of scenario earthquakes using this relation are shown on Figure E-1. A description of the cyclic stress method and the results using liquefaction potential analysis are provided also in Appendix E (Table E-1, Table E-2, Table E-3, Table E-4, and Table E-5). The magnitude-distance relation requires measured distances between possible source areas and liquefaction features and liquefaction potential analysis requires measured distances between possible source areas and locations of geotechnical data used in the analysis. These distances were measured within the project ArcGIS framework. The same geotechnical data gleaned from borehole logs for the initial assessment of sedimentary

conditions along rivers was used in the liquefaction potential analysis (Table B-2 and Table B-3). In central Virginia river valleys, the water table typically occurs within a meter of the ground surface, but can drop several meters during periods of drought (Kempthorne and Myers, 2006; USGS website https://waterdata.usgs.gov/nwis/gw). Also, lower relative sea level in the past may have affected the water table particularly in the Coastal Plain (Van de Plassche, 1990; Cohen et al., 2022). Therefore, water table depths of 1 m and 3 m were used in most of the analyses, though only 1 m water table depth was used in the analyses for historical scenario earthquakes.

4 SELECTION OF RIVER SEGMENTS FOR SURVEYS OF LIQUEFACTION FEATURES

The selection of study areas or river segments for surveys for earthquake-induced liquefaction features is a critical task in any paleoliquefaction study (e.g., Tuttle et al., 2018 and 2019a). Efforts must be made to maximize the chance of finding features and to collect a representative sample of liquefaction field data so that the results will be as meaningful as possible. The selection process is based on identifying areas where sedimentary conditions exist for the formation and preservation of liquefaction features and where exposure is adequate to find the features, if they are present. Conditions necessary for the formation of features include the presence of loose to moderately loose, sandy deposits that tend to be susceptible to liquefaction overlain by less permeable silty and clayey deposits that promote the buildup of pore-water pressure during ground shaking. The sandy deposits must be below the water table or water-saturated at the time of the earthquake for liquefaction to occur. In order for the features to be preserved they must exist in a relatively stable environment where the geologic record has not been destroyed by natural events or human activities. In the CVSZ, Holocene and Late Pleistocene (0.129 to 0.0117 Ma; Cohen et al., 2022) alluvium, which is often susceptible to liquefaction, underlies flood plains and are exposed along rivers flowing out of the Appalachian Piedmont and across the Coastal Plain. Therefore, rivers in and around the CVSZ offer the opportunity to search for and study the liquefaction record of past earthquakes in the region.

4.1 Review of Surficial Geology

In order to identify areas where sedimentary conditions are conducive to the formation of liquefaction features during strong ground shaking, geological maps and reports relevant to the Quaternary geology of the study region were reviewed. In particular, the geological maps of the Coastal Plain and adjacent areas of the Piedmont, the Fredericksburg $30' \times 60'$ quadrangle, and the Colonial Beach 7.5' quadrangle were very useful (Mixon et al., 1989 and 2000; Newell et al., 2006). Holocene and Pleistocene alluvium and upper to middle Pleistocene deposits, primarily of the Tabb and Shirley Formations, are mapped along portions of the Mattaponi, Potomac, Rapidan, and Rappahannock Rivers (Table B-1). With the exception of cobbly and bouldery sediment, flood plain deposits characterized by interbedded coarse- and fine-grained sediment might be promising for finding liquefaction features. Cobbly and bouldery sediment is very difficult to liquefy and therefore are unlikely to contain liquefaction features unless subjected to very large earthquakes (Tuttle et al., 2017).

Along the Mattaponi from Milford downriver to the Rt. 301 bridge and also farther downstream from the Rt. 628 bridge near Beulahville to the Rt. 360 bridge near Aylett, Holocene and Pleistocene alluvium consists of fine to coarse gravelly sand, sandy gravel, silt, and clay deposited in channel, point-bar, and flood plain environments. In addition, Pleistocene alluvial terrace deposits also composed of fine to coarse gravelly sand, sandy gravel, silt, and clay are mapped along these two river segments.

Holocene and Pleistocene alluvium, very similar to that along the Mattaponi, is mapped along the Rappahannock River from Fredericksburg to Port Royal. In addition, upper Pleistocene, Tabb Formation and middle Pleistocene, Shirley Formation are mapped along the river. The Tabb Formation is composed of sand, gravel, silt, and clay and underlies low terraces. The Shirley Formation consists of fine to coarse sand, in part pebbly and boulder, grading upward to silty fine sand and sandy silt, filling fluvial channels.

Along the Virginia shoreline of the Potomac River, Holocene marsh deposits of silt, clay, mud, muddy sand, and sand are mapped along the margins of estuaries of Upper Machodoc and Popes Creeks. In addition, the middle Pleistocene, Shirley Formation is mapped near the mouth of Potomac Creek, and the upper Pleistocene, Tabb Formation is mapped in the Mathias Point area and downriver to the Popes Creek area.

Along the Rapidan River, Holocene and Pleistocene alluvium composed of gravel, sand, silt, and clay, and including coarse-grained channel fills overlain by fining-upward sequences, are mapped beneath modern flood plains. In addition, Pleistocene/Pliocene terrace deposits of gravel, sand, silt, and clay are mapped below lowland benches above and adjacent to the modern flood plains.

It appears that the surficial geology has not been mapped along the Appomattox River west of the Fall Line; however, the sediment is likely to be similar to Holocene and upper Pleistocene sediment along the South Anna River where it crosses the Appalachian Piedmont (Pazzaglia et al., 2015 and 2021; Tuttle et al., 2021). The South Anna alluvium consists of sand and gravel with variable amounts of silt and clay and include modern alluvial deposits as well as former alluvial deposits that occur above the modern flood plain and underlie terrace landforms (Malenda et al., 2014).

4.2 Review of Geotechnical Data

Suitable conditions for the formation of earthquake-induced liquefaction features include saturated sandy sediment with loose to moderate relative density that occurs below a low-permeability layer of silt or clay and less than 16 m below the surface (e.g., Tuttle et al., 2018 and 2019a). To help identify areas with suitable conditions, geotechnical data were reviewed that were available through the Virginia Department of Transportation. These data included borehole logs and cross-section for bridge crossings of the Mattaponi, Rappahannock, Potomac, Rapidan, and Appomattox Rivers Figure 2-1). Prior to this project, geotechnical data were reviewed for the Rivanna, South Anna, James, and Pamunkey Rivers and for an upstream portion of the Mattaponi River (Tuttle et al., 2021). Potentially liquefiable layers were identified at all the locations listed in Table B-2. Representative layers and their characteristics are summarized in Table B-3. They include sandy sediment with standard penetration test (SPT) blow counts (N), a measure of soil density, mostly between 2 and 11, but ranging up to 22 that occur at depths less than 11 m below the natural ground surface. The sandy layers were overlain by clay, silty clay, silt, or sandy silt, and the water table was often within several meters of the ground surface.

Unfortunately, there was no geotechnical data available for Rt. 628 bridge crossing of the Mattaponi River near Beulahville. However, there was data available for the Rt. 360 bridge crossing of the river in Aylett (Figure 2-1; map ID 9). At Aylett, borehole logs indicate limited sedimentary conditions conducive to the formation of earthquake-induced liquefaction features. In one of five boreholes, sandy clay is interbedded with gray sand with organics between 2.5-3.7 m BS. Blow counts in the gray sand range from 19-22, indicating that the sand is moderately dense. Most of the other borehole logs show 7.3-8.2 m of very loose to loose, brown and gray sand with organics and gray sand with gravel underlain by 12.5-13 m of gray-dark gray silt with mica and shells. According to these other logs, there is no capping layer of silt or clay overlying the very loose to loose sand.

Borehole logs for the Rt. 3 bridge crossing the Rappahannock River near Fredericksburg show sedimentary conditions conducive to the formation of liquefaction features, including two layers of loose sand both overlain by fine-grained layers (Figure 2-1; map ID 10). More specifically, the logs show 1.8-2.7 m thick layer of brown sand with organics overlain by silty-sandy clay and a

deeper layer 0.9-1.2 m thick of gray sand overlain by silty clay. The upper layer has a blow count of 5, whereas the lower layer has a blow count of 7. Downstream at Port Royal, borehole logs for the Rt. 301 crossing of the Rappahannock River show sedimentary conditions less than ideal for the formation of liquefaction features (Figure 2-1; map ID 11). The logs reveal a section, 12-19.5 m thick, of mostly clay and clayey silt both with shells. Only one of the logs shows loose (N=7), silty sand, 0.9 m thick, sandwiched between sandy clay and clayey silt.

No borehole logs were examined for the Potomac River itself. However, borehole logs were examined for bridge crossings of two tributaries of the Potomac River including Williams Creek and Tide Mill Stream (Figure 2-1; map ID 12 and 13, respectively). Sedimentary conditions appear to be suitable for the formation of liquefaction features at both locations, though loose sand at Williams Creek is more susceptible to liquefaction than the moderately dense sand at Tide Mill Stream. Borehole logs for the Rt. 206 bridge crossing of William Creek reveal 14-15 m of sandy silt and clay underlain by 4.9-8.5 m of gray sand. The upper portion of the gray sand is often loose to moderately dense (N=7-14) and the lower portion of the sand is dense (N=31-50). Borehole logs for the Rt. 205 bridge crossing of Tide Mill Stream show two layers of silty, fine sand both overlain by clay. The upper silty sand encountered at 1.5 m depth is 0.6 m thick and the lower silty sand encountered at 4.3 m depth is at least 0.5 m thick; both sand layers are moderately dense (N=15-20).

Sedimentary conditions appear to be suitable for the formation of liquefaction features along the Rapidan River, too. Borehole logs for Rt. 522 bridge crossing of the river (Figure 2-1; map ID 14) near Racoon Ford show 0.6-1.5 m of silt with trace of sand underlain by 1.0-1.4 m silty fine sand with gravel at the base of the unit. Blow counts vary from 4-22 with the higher value only in the gravelly portion of the deposit, indicating that most of the deposit is loose. Bedrock was often encountered within 5.5 m below the surface (BS).

Borehole logs for the Rt. 609 bridge crossing the Appomattox River south of Macon suggest nearly ideal sedimentary conditions for the formation of earthquake-induced liquefaction features (Figure 2-1; map ID 15). Several of the logs show underlain by 1.2-3.2 m of silty, fine-medium sand or silty, fine-coarse sand coarse sand overlain by 0.6-1.5 m of silty clay or sandy clay. Blow counts in the silty sand range from 2-9, indicating that the sand is very loose to loose. Bedrock was often encountered within 6 m BS.

4.3 Review of Satellite Imagery

Except for urban and suburban areas, much of the study region is heavily forested and vegetated. Even in agricultural areas where trees have been removed for growing crops, forested buffer zones have been left along river banks. Satellite imagery acquired during leaf off provided the best views of the river banks. Even so, it was difficult to evaluate cutbank exposure along most of the rivers due to forest cover (Table B-1). Satellite imagery was useful for identifying access points, especially along the Mattaponi, Rapidan, and Appomattox Rivers where there are long distances between bridge crossings and few public boat or canoe ramps.

Reviewing Google Earth (GE) satellite imagery acquired of the Mattaponi River, both segments from Milford to the Rt. 301 bridge and from the Rt. 628 bridge near Beulahville to the Rt. 360 bridge near Aylett were heavily forested. Along the upstream segment, no cutbank exposures could be seen through the trees and there appeared to be many downed trees in the stream. Along the downstream segment, a few cutbank exposures could be seen in river bends.

On GE satellite imagery of the Rappahannock River from Fredericksburg to Port Royal, most banks appeared heavily forested or otherwise vegetated. There were a few exposures in river bends, especially in the large bends around Skinker's Neck. In addition, there appeared to be a few bank failures or slumps downriver from Fredericksburg, along the southwestern bank of the river in the vicinity of the Fredericksburg Country Club, near Belvedere Drive and Gravel Pit Farm Road, along the northern river bend around Skinker's Neck, as well as upriver and downriver from Hopyard landing (boat ramp) and Hick's landing.

On GE imagery, there appeared to be very good to excellent exposure along the southern shoreline of the Potomac River along the northern and eastern sides of Mathias Point, near Dahlgren Navy Base, south of Potomac Beach, and north of Popes Creek. There were retaining walls, riprap, and groins to protect banks from erosion in places along the north and east sides of Mathias Point, at Colonial Beach, and at a community south of Popes Creek. There also appeared to be a few cutbank failures in (1) Upper Machodoc Creek estuary along the west bank of Williams Creek and near Dahlgren Navy Base; (2) Rosier Creek estuary along the north shore; Popes Creek estuary along both the northern and southern shores.

On GE imagery of the Rapidan River from the town of Rapidan past Racoon Ford, there appeared to be small cutbank exposures in river bends and slump scarps along the mostly forested and otherwise vegetated banks. Most of the exposures occurred along portions of the river flanked by roads both north and south of the Rt. 522 bridge.

GE imagery of the Appomattox River was reviewed from the Farmville area to the Genito area. Almost the entire length of the river is heavily forested with a few cutbank exposures visible in river bends. In the Farmville area, where there is development along the river, cutbank exposures appear to be slightly more common.

4.4 Inspection of River Segments

As mentioned above, Holocene and Pleistocene alluvium are mapped along portions of the Mattaponi, Rappahannock, Potomac, and Rapidan Rivers and sedimentary conditions appear to be conducive to the formation of earthquake-induced liquefaction features along portions of these rivers. Therefore, field inspections of selected river segments were performed at bridge crossings, along roads that pass close to the rivers, and at public access points to further evaluate surficial geology, exposure, and access.

The Mattaponi River was examined at the Nelson Hill Road bridge crossing near Milford as well as a public landing upriver from the bridge. Attempts were made to view the river farther downstream but access roads were gated and posted. At the two locations where the river was viewed near Milford, the banks were very low and there was no exposure. On the 7 ½ minute Woodford topographic quadrangle of the area, there is little to no relief along the river and much of the flood plain is mapped as marshland. On the 7 ½ minute Penola topographic quadrangle to the southeast, relief along the river increases to 3-6 m and only old courses of the river are mapped as marshland. Therefore, cutbank exposures may be more likely along this portion of the river. However, none were observed on satellite imagery and access appears to be very limited. Therefore, the Mattaponi River also was inspected farther downstream from a previously surveyed segment of the river along which liquefaction features were found. At the Rt. 628 bridge crossings near Beulahville, cutbank exposures of sandy and silty sediment could be seen in the 5-6 m high banks. Farther downstream on the Rt. 301 bridge in Aylett, traffic was too busy to view the river and its banks. At a public boat ramp nearby, the river banks were heavily vegetated.

The Rappahannock River was viewed at the Fredericksburg boat ramp, Little Falls boat ramp, boat ramp at Four Winds campground, Hopyard landing, Hick's landing, and Port Royal landing. Across and downstream from the Fredericksburg boat ramp, river banks are fairly high and steep but there were no apparent exposures. From the Little River boat ramp, a bank failure could be seen across that provided a 3-4 m high exposure of sand fining upward to silt and clayey silt. The owner of Hick's landing reported that 1-2 m cutbanks are exposed at low tide upriver and downriver from the landing. At the Four Winds campground, river banks were low and afforded no exposures. At Hopyard and Hick's landings, a few cutbank exposures were visible in the two lowest terraces and the boat ramps provide access to the river. At Port Royal, the river banks were very low and marshy.

The Potomac River and several tributaries were examined at Popes Creek landing, at George Washington Birthplace National Monument, Bridges Creek landing, Stepp's Harborview Marina and Harborview Circle on Mattox Creek, Rt. 205 or Ridge Road on Rosier Creek, Berry Wharf Road on Upper Machodoc Creek, Fairview Beach Yacht Club, and Waugh Point Marina on Potomac Creek. Many of the roads on Mathias Point Neck are private so access to the Potomac River is very limited there. At Caledon State Park west of Mathias Point Neck, an onsite map indicates a canoe landing on the Potomac River. Cutbank exposures 3-4.5 m high were observed along the Potomac River south of Popes Creek as well as north and south of Bridges Creek. The exposures revealed 1-1.5 m of loose interbedded silt and sand with pebbles and cobbles in which several paleosols had formed, overlying 2-3 m of massive gray sandy silt to clayey silt with iron-stained, subparallel joints. Several 3 m high exposures of similar deposits were observed in Popes Creek estuary and one exposure was observed in Rosier Creek estuary. Holocene estuarine and fluvial deposits dating back 6,000 yr (Newell et al., 2006) have been mapped in the estuaries though no exposures in these deposited were observed during reconnaissance.

The Rapidan River was examined from the bridge crossing in the town of Rapidan, along roads which follow portions of the southern bank of the river, and at Raccoon Ford. The river can be accessed from these locations. Several access roads were gated and posted; however, permission was gained from several property owners to access the river through their property. River banks were 1.5-2.5 m high and mostly vegetated. Several exposures between Rapidan and the Rt. 522 bridge revealed silty sand. The most extensive exposure was between the Rt. 522 bridge and Racoon Ford and revealed reddish clayey silt.

The Appomattox River was viewed at the Rt. 609 and Rt. 604 bridge crossings near Macon and Genito, respectively, and from several private roads that came close to the river. There was poor river access at the bridge crossings; however, several property owners granted access. The upper portions of the 3-4 m high river banks were vegetated, but the lower portions of banks were exposed, revealing mottled silt and silty sand.

4.5 Selection of River Segments

Due to poor exposure and access, the segment of the Mattaponi River between Milford and the Rt. 301 bridge was not selected for river survey. Instead, the segment of the Mattaponi between the Rt. 628 bridge near Beulahville and Rt. 301 bridge in Aylett was selected since sedimentary conditions and exposure appear to be adequate. In addition, surveying this segment of the river extends the search for liquefaction features towards the east beyond previously found liquefaction features on the Mattaponi.

Along much of the Rappahannock River between Fredericksburg and Port Royal, cutbank exposure of Holocene and upper Pleistocene deposits appeared to be very limited. Exposure

was especially poor along the lower 7 km of the river, except for cutbanks in older deposits underlying a high terrace. Nevertheless, the segment of the river from Fredericksburg to Hick's landing was selected for survey since the Rappahannock is 30-40 km north of the portion of the Mattaponi River where liquefaction features previously were found. Also, this segment of the Rappahannock River crosses the trace of the Skinker's Neck fault zone.

Exposure was excellent along portions of the Potomac River and fairly good along the estuaries of Popes and Upper Machodoc Creeks, but sedimentary conditions conducive to the formation of liquefaction features is very sparse. A few Holocene deposits appeared to occur along the banks of the estuaries. Navigating the Potomac River can be tricky given its currents and tides as well as its large fetch subject to strong winds and substantial waves. Therefore, short stretches of exposures of the Potomac in the vicinity of Popes and Bridges Creeks were selected for survey on foot. In addition, estuaries of Popes, Rosier, and Upper Machodoc Creeks, protected from winds and waves, were selected for survey. Boating activity in Popes Creek estuary is restricted because it is part of the George Washington Birthplace National Monument. Permission to work in Popes Creek estuary was requested from and granted by the National Park Service.

Although exposure of Holocene and Pleistocene alluvium appeared to be limited along the Rapidan River, the segment from the town of Rapidan to a take out on a farm northeast of Racoon Ford was selected for survey. Surveying this portion of the river extends the search for liquefaction features north of the CVSZ.

A segment of the Appomattox River was selected for survey from an access point near the Rt. 609 bridge crossing south of Macon to an access point at the mouth of Rocky Ford Creek. Both access points as well as one in between were on private property where permission was granted for us to work. This segment was selected for survey because sedimentary conditions appeared to be almost ideal for the formation of liquefaction features and exposure of Holocene and upper Pleistocene deposits looked to be fairly good. This segment of the river is only ~20 km from liquefaction features previously found on the James River and not far from the southern trend line of the Hylas fault. In addition, surveying the Appomattox extends the search for liquefaction features towards the southern margin of the CVSZ.

5 RIVER SURVEYS FOR LIQUEFACTION FEATURES

As discussed in Section 4, river segments were selected for surveys on the basis of the review of surficial geology, borehole data, satellite imagery, and reconnaissance of field conditions. Surveys of all rivers were conducted during relatively dry periods when river levels were low in order to maximize cutbank exposures of Holocene and upper Pleistocene deposits and chances of finding liquefaction features, if they were present. For tidal portions of rivers, the surveys were conducted also during periods of especially low tides.

In October 2021, surveys were conducted along the Mattaponi River downstream from a previously searched segment of the river where liquefaction features were found, a short segment of the Potomac River and several tributaries to the Potomac River, and the Rapidan River downstream from the town of Rapidan (Figure 2-1). In June and September 2022, the Rappahannock River was surveyed between Fredericksburg and Hicks landings located about 7 km upstream from Port Royal. Also in September 2022, the Appomattox River was surveyed downstream from Rt. 609 bridge south of Macon (Figure 2-1). A summary of conditions and findings along the rivers is presented in Table 5-1, information gathered at study sites is summarized in Table C-1, and results of C14 and OSL dating are provided in Appendix D.

5.1 Mattaponi River

The survey for liquefaction features was conducted along 24.5 km of the Mattaponi River from the Rt. 628 bridge near Beulahville to the public boat ramp in Aylett. Surficial geology of this stretch of the Mattaponi River is mapped as Holocene and Pleistocene alluvium (fine to coarse gravelly sand and sandy gravel, silt, and clay); upper Pleistocene Tabb Formation, Sedgefield member (pebbly to bouldery, clayey sand and fine to medium shelly sand, grading upward to sandy & clayey silt) at altitudes of 6-9 m; middle Pleistocene Shirley Formation, (sand, gravel, silt, clay, and peat) at altitudes of 10-14 m; lower Pleistocene, Charles City Formation (sand, silt, and clay) at altitudes 21-24 m; and upper Pliocene to lower Miocene, Chesapeake Group (fine to coarse sand, silt and clay, marine bones and shark teeth, planar joints) (Mixon et al., 1989).

During the survey, it was found that at least three terraces occur along this segment of the river. Most cutbank exposures occurred in the lower two terraces about 1.5-3 m and 5-6 m above the river level, and there were several exposures in the highest terrace about 20 m above the river level (Table 5-1). Most river banks were vegetated or covered with organic debris from recent floods; however, there were numerous eroding cutbanks mostly in river bends. Recent point bar deposits of interbedded silt and pebbly sand were draped on lower cutbanks and were most common along the 5 km stretch upstream from the mouth of the Herring Creek.

Sediment exposed in cutbanks of the lowest terrace includes sand underlain by mottled gray and yellowish-orange silt followed by interbedded pebbly sand, silty very fine sand, sandy silt, and silt (Table C-1). The silty sand towards the bottom of the cutbanks appeared to be very susceptible to liquefaction. Probing below the water level, interbedded silt and sand continued for at least another 1.5 m. Occasionally, dense silt was encountered at 0.5 m below the water level. C14 dating of MR200-C1 collected about 25 cm above the water level from sand yielded a calibrated age of 490-420 and 411-315 yr B.P. (Table D-1). The date suggests that much of the sediment exposed in cutbanks of the lowest terrace was deposited in the past 550 years.

Table 5-1: Summary of River Surveys - Exposure, Conditions, and Earthquake-Induced Liquefaction Features

River Surveys	Cutbank Exposure	Suitable Conditions	Sediment Age*	Liquefaction Features	Estimated Feature Age
Eastern CVSZ					
Mattaponi 24.5 km	Good in lower two terraces (1.5-3 m & 5-6 m) in river bends along 15 km downstream from Rt. 628 bridge	Yes, but limited; Holocene and upper Pleisto-cene alluvium; interbedded sand, silt, & clay	Holocene terrace (1.5-3 m): 490 yr BP; upper Pleistocene terrace (5-6 m): 38,470 yr BP	None	Not applicable
Northeastern CVSZ					
Rappahannock 40 km	Overall poor – most banks vegetated & protected with riprap; few cutbanks in 4 terraces	Yes, but very limited; Holo-cene alluvium (1-2 m terrace); reddish brown, silt with inter-beds of sand	Modern terrace (1-2 m): 100 yr BP	None	Not applicable
Potomac & Potomac Estuaries 11 km	Excellent along Potomac; good in Popes and Upper Macho-doc estuaries; poor in Rosier estuary	Hardly; Holo-cene alluvium - very sparse; upper Pleisto-cene sandy deposits occur high in section & rarely with capping layer	Probably from Calvert Formation: >43,500 yr BP	None	Not applicable
Northern CVSZ					
Rapidan 23 km	Fair; few exposures in 3-4.5 m terrace in cutbanks in river bends & slump scarps	Yes, Holocene alluvium but only 6 m thick; interbedded silt & sand or silt with interbeds of sand	Holocene terrace (3-4.5 m): 1830 yr BP	SSDs at two sites and one small sand dike	Historical or prehistorical: 1830-60 yr BP
Southern CVSZ					
Appomattox 8 km	Good to excellent in most river bends, 4-5 m high	Yes, nearly ideal; Holocene & upper Pleisto-cene alluvium; inter-bedded silt & sand	Holocene & upper Pleisto-cene terrace (3-4 m): 2,450-27,520 yr BP	Unweathered sand dikes; weathered sand dikes & intruded krotovinas	Historical; prehistorical: 3,450-2,450 yr BP

***** Sediment ages (rounded to nearest decade) of samples collected from river cutbanks; may not reflect the maximum age of sediment exposed or underlying the cutbanks.

Figure 5-1: Photographs at site MR201 of cutbank exposure in 6-m-high river terrace along Mattaponi River: (left) exposure is very good of lower portion of cutbank; black rectangle outlines area of closeup photo; (right) annotated closeup of bioturbated and mottled silty sand overlying brownish, clayey silt with subvertical joints. C14 dating of sample MR201-S1 indicates mottled silty sand is upper Pleistocene in age. Underlying clayey silt is probably member of Chesapeake Group. For scale, black and white intervals on hoe handle are 25 cm long.

Sediment exposed in cutbanks of the 5-6 m-high terrace includes sand underlain by bioturbated and mottled silty sand followed by grayish olive and dark olive gray, clayey silt characterized by subparallel high-angle fractures (Table C-1). In places, the clayey silt appears to have been laminated and bioturbated. Probing below the water level, clayey silt continued for 0.25-0.5 m and was underlain by at least 1-1.25 m of sand. At site MR201, a sample of organic sediment, MR201-S1, collected from the bioturbated and mottled silty sand about 4.1 m below the top of the cutbank and 10 cm above the contact with clayey silt yielded a calibrated C14 age of 38,474-36,679 yr B.P. (Figure 5-1). A vertebra of marine mammal, probably a dolphin (M. Rathgaber, pers. comm., 2021), was found in the silty sand about 10 cm above sample MR201-S1. The bone was too degraded and contained too little collagen to be dated but was likely reworked from older deposits containing marine fossils. The section exposed in the 5-6 m-high terrace may be composed of Pleistocene alluvium overlying members of the Chesapeake Group.

Sediment underlying the highest terrace, about 20-m high, includes pale yellowish orange, grayish olive, and dark olive gray, dense clayey silt. Downstream from Herring Creek to the Aylett boat ramp, a distance of about 8 km, the river passes through a marshy area where most banks are only 1-2 m high, vegetated, and covered with woody debris. In addition, there are several high banks probably in the 20-m high terrace. Exposures in both the 2-m high banks and in the lower 2 m of the 20-m high banks reveal dark olive gray, clayey silt with high-angle fractures. This sediment is likely representative of the Chesapeake Group.

Sedimentary conditions conducive to the formation of liquefaction features (e.g., interbedded sand, silt, and clay) are fairly common in 1.5-3 m high terrace along the 15 km downstream from the Rt. 628 bridge near Beulahville and are present in the 5-6 m terrace, but more limited especially along the lower 8 km in the vicinity of Aylett. No earthquake-induced liquefaction feature was observed in sediment of either terrace level. Exposed sediment of the 1.5-3 m high terrace appears to be 550+ yr old; whereas, exposed sediment of the 5-6 m terrace is as much as 38 kyr (thousand years) old. Therefore, the younger alluvium has the potential to record historical earthquakes; whereas, the older alluvium has the potential to record upper Pleistocene and Holocene earthquakes so long as the water table was high enough to saturate liquefiable sediment at the time of the event.

5.2 Rappahannock River

The survey for liquefaction features was conducted along 40 km of the Rappahannock River from the Rt. 3 bridge in Fredericksburg downstream to Hick's landing which is 7 km short of Port Royal (Figure 2-1). Between the Rt. 3 bridge and Skinker's Neck where the river is crossed by the Skinker's Neck fault zone, the surficial geology is mapped as Holocene and Pleistocene alluvium (fine to coarse gravelly sand and sandy gravel, silt, and clay); upper Pleistocene Tabb Formation (sand, gravel, silt, and clay underlying low terraces); and middle Pleistocene Shirley Formation, (pebbly and bouldery, fine to coarse sand, grading upward to silty fine sand and sandy silt) (Table B-1; Mixon et al., 2000). Between Skinker's Neck and Hick's landing, the surficial geology is much the same but also includes the Sedgefield Member of the Tabb Formation (pebbly to bouldery, cross-bedded, fine to coarse sand, grading upward to sandy and clayey silt).

During the survey, at least four terrace levels were noted along the river: 1-2 m, 4-5 m, 7-8 m, and 16-18 m above the river level. Overall, exposure was poor with many banks heavily vegetated and some banks protected from erosion with riprap (Table 5-1). The few cutbank exposures occurred in river bends and most notably in the large river bends around Skinker's Neck. Along the upper 15 km of the river segment, a few cutbank exposures occurred in the 1-2 m, 4-5 m, and 16-18 m terraces; whereas along the lower 25 km, cutbank exposures were more frequent in the 1-2 m and 7-8 m terraces, with a few exposures in the 16-18 m terrace. Cutbanks in the 1-2 m terrace revealed tan, sand or sandy silt underlain by reddish brown, silt or sandy silt with thin interbeds of sand. Probing below the water level, silt with interbedded sand, 5-10 cm thick, continued to at least 1.5 m depth. The few cutbanks in the 4-5 m terrace exposed reddish, sandy silt. The more numerous cutbanks in the 7-8 m terrace revealed mostly pebbly sand overlying dark gray, silty sand sometimes containing shells. The few cutbanks in the 16-18 m terrace exposed pebbly sand or pebbles overlying dark gray silt sometimes with layering.

Study sites RkR1 and RkR2 were in the lowest terrace (Table C-1). At RkR1, the cutbank was 1.1 m high and exposed tan, sand overlying reddish brown, very fine sandy silt with a 2-3 cm thick layer of silty sand. Probing below the water level, silt with interbeds of sand up to 10 cm thick continued to 1 m depth followed by silt to 1.5 m. At RkR2, the cutbank was 2 m high and exposed a thin veneer of recent very fine sand over tan, coarse to very fine sandy silt underlain by reddish brown, silt (Figure 5-2). Probing below the water level, silt with interbeds of sand up to 5 cm thick continued to 1.5 m depth. Sediment samples for OSL dating were collected 1.1 m BS from the tan, coarse to very fine sandy silt and 1.6 m BS from the reddish brown, silt. Both samples gave very young ages, with the sample RkR2-OSL2 collected lower in the section giving a slightly older age of 100-80 yr B.P. (Table D-2).

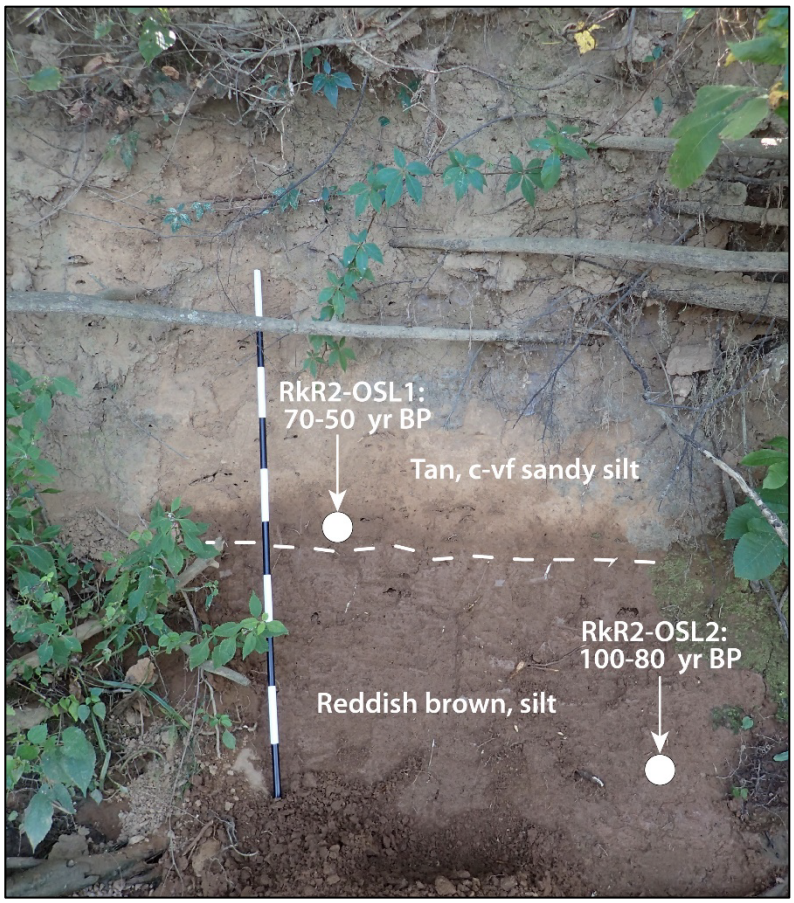

Figure 5-2: Photographs at site RkR2 of cutbank exposure in lowest (1-2 m) river terrace along Rappahannock River. Cutbank revealed tan, sandy silt underlain by reddish brown, silt. OSL dating of sample OSL2 suggests that the exposed sediment is very young. Probing to 1.5 m depth below the water level, sand layers up to 5 cm thick occur within silt. For scale, black and white intervals on meter stick represent 10 cm.

Sedimentary conditions conducive to the formation of liquefaction features (e.g., interbedded sand, silt, and clay) appear to occur in sediment underlying the lowest terrace. Unfortunately, there were few exposures of sediment of the lowest terrace. In addition, OSL dating suggests that the sediment is very young, too young to record earthquakes that induced liquefaction more than 150 yr ago or prior to A.D. 1850.

5.3 Potomac River and Upper Machodoc, Rosier, and Popes Creeks

Surveys for liquefaction features were conducted along a stretch of the south bank of the Potomac River northwest of the mouth of Popes Creek and in estuaries of Popes, Rosier, and Upper Machodoc Creeks (Figure 2-1). The surveys were conducted along 1.2 km of the Potomac River shoreline, including three short sections accessed by foot, as well as 3.9 km, 1.1 km, and 4.8 km of the estuarine shorelines of Popes, Rosier, and Upper Machodoc Creeks, respectively, that were accessed by canoe. Exposure was excellent along the shoreline of the Potomac River, good along the banks of Popes Creek and Upper Machodoc Creek estuaries, and poor along the banks of Rosier Creek estuary (Table 5-1). The northwestern shore of Popes Creek estuary and

the adjacent shoreline of the Potomac River are within the George Washington Birthplace National Monument (GWBNM) and a research permit was granted to work within the monument.

Mapped surficial geology of the three areas includes Holocene marsh deposits (organic-rich silt, clay, and sand), upper Pleistocene Tabb Formation (pebbly sand and sandy silt) including the Sedgefield and Lynhaven members, as well as upper Pliocene and lower Miocene Chesapeake Group which underlie the Quaternary deposits (Table B-1; Mixon et al., 2000; Newell et al., 2006).

Along the Potomac River, there were 3-3.5 m high cutbanks that provided exposure of partially covered reddish, fine sandy silt underlain by greenish-gray, fine sandy silt, followed by brownish, clayey silt with organics atop gray, silt with iron-cemented subparallel joints (Figure 5-3. The brownish, clayey silt may represent a paleosol and C14 dating of sample PPC2-C1 from the horizon suggests that the sediment was deposited more than 43 ka (thousand years ago) (Table C-1 and Table D-1). Close to the mouth of Popes Creek, cutbanks revealed parallel-bedded, pebbly sand underlain by gray and yellowish orange, massive silt, followed by gray and yellowish orange, clayey silt (Figure 5-4).

The geologic section exposed along this portion of the Potomac River represents upper Pleistocene Tabb Formation overlying the Calvert Formation of the Lower Chesapeake Group (Newell et al., 2006). Holocene organic-rich silt, clay, and sand occur in only a few locations, near the mouth of Popes Creek and the mouths of Digwood Swamp and Bridges Creek where they meet the Potomac.

Figure 5-3: Photograph of almost continuous cutbank exposure along Potomac River northwest of Popes Creek estuary. Along base of cutbank, gray silt characterized by cemented, subparallel, high-angle joints probably is part of the Calvert Formation, a member of lower Chesapeake Group.

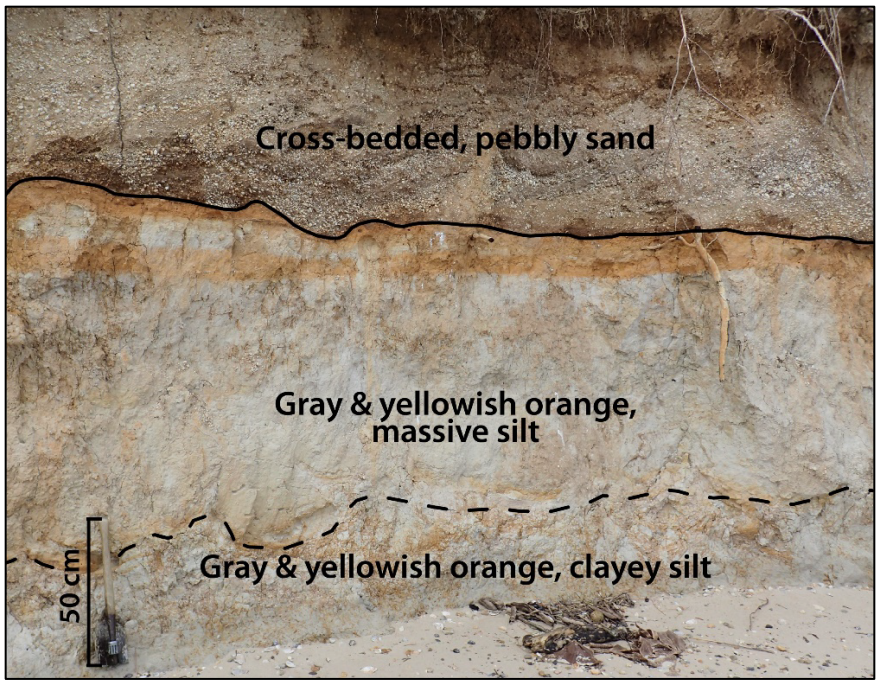

Figure 5-4: Photograph at site PPC3 of cutbank exposure along Potomac River near mouth of Popes Creek. Cross-bedded pebbly sand is probably upper Pleistocene Tabb Formation and unconformably overlies gray and yellowish orange silt and clayey silt of Calvert Formation.

Along the northwest shoreline of Popes Creek estuary, banks were 2-4 m high and mostly vegetated. Several cutbanks revealed iron-stained, silt underlain by gray, silt. One exposure of the lower two meters of a 4-m high bank revealed pebbly sand. Along the southeast side of the estuary, banks were 2-7 m high. Cutbanks were more numerous and revealed 2-5 m of gray, silt. Close to the mouth of the estuary, iron-stained, pebbly sand again was observed overlying gray and pinkish gray, silt. Similar to the geologic section along the nearby segment of the Potomac River, the section exposed in Popes Creek estuary also represents upper Pleistocene Tabb Formation overlying the Calvert Formation (Newell et al., 2006).

Along Rosier Creek estuary, there were banks up to 4.5 m high but they are mostly vegetated. Along the northwest side of the estuary, there was one exposure of pebbly sand in the upper portion of the bank and another exposure of gray, silt towards the bottom of the bank. Near the mouth of the creek, organic-rich silt and white sand recently had been deposited against the lower portion of the bank. There were no exposures along the southeast bank of the estuary which is more heavily developed.

Along the northwest side of Upper Machodoc Creek, banks were 1.5-3.5 m high and mostly vegetated. A few cutbanks exposed reddish, silt with thin layers of sand overlying reddish and gray, silt with layers of sand and sandy silt. Along the southeast side of the estuary, banks were mostly 4.5-5 m high with more numerous cutbank exposures of reddish, silt with lenses of pebbly sand, probably channel deposits, overlying gray, silt with layers of sand and sandy silt. At Howland Point along the southern shore of the estuary, cutbanks in a low terrace about 1 m high revealed tan, silt overlying brownish, pebbly silt. The geologic section exposed in Upper Machodoc Creek estuary likely represents predominately upper Pleistocene Tabb Formation, including the Sedgefield Member, overlying members of the Chesapeake Group. Holocene marsh deposits of silt and pebbly silt occur below a few low terraces.

No earthquake-induced liquefaction features were found in sediment exposed along the Potomac River or estuaries of Popes, Rosier, and Upper Machodoc Creeks. However, sedimentary conditions suitable for the formation of liquefaction features are few and far between in these areas. Along the Potomac-Popes Creek area, upper Pleistocene sandy deposits occur high in the section but capping, low-permeability layers are rare. In the Upper Machodoc Creek estuary, upper Pleistocene deposits include interbedded silt and sand but they also occur high in the section. These deposits have the potential to record upper Pleistocene and Holocene earthquakes but the water level would have to be very high to saturate the deposits at the time of the event. Holocene deposits which are likely to be susceptible to liquefaction are unfortunately very sparse.

5.4 Rapidan River

The survey for liquefaction features was conducted along 23 km of the Rapidan River from the bridge crossing in the town of Rapidan to an access point on a farm northeast of Racoon Ford. Along this segment of the river, Holocene and Pleistocene alluvium, about 6 m thick, includes fining-upward sequences of gravel, sand, silt, and clay underlying the modern flood plain (Table B-1; Mixon et al., 2000). Pleistocene/Pliocene terrace deposits, up to 10 m thick, includes gravel, sand, silt, and clay underlying lowland terraces that are 6-20 m above the adjacent modern flood plains. Modern point bars occur more commonly along the upper 12 km than the lower 11 km of the river segment.

During the survey, two terrace levels were noted along the river. There were relatively few cutbank exposures, most of which occurred in river bends and in the lower terrace, which was 3-4.5 m above the river level (Table 5-1). Usually, the upper portions of the banks were vegetated and exposures occurred in the lower half or third of the banks. There were a few slump scarps that exposed the upper half to two-thirds of the bank with the lower portion of the bank covered by the slump. Most exposures revealed interbedded silt and iron-stained sand or mottled silt with a few thin layers of sand. Occasionally, sandy silt or pebbly sand with few cobbles occurred near the base of the cutbank. Probing below the water level, silt or interbedded silt and sand continued for only 0.5-1.5 m where bedrock was almost always encountered.

Soft-sediment deformation structures (SSDs) were found at two sites along the river, RnR1 and RnR2 (Table C-1). At site RnR1, deformation structures included pseudonodules or rounded masses of sand extending downward into the underlying silty sand layer and diapirs of the silty sand extending into the overlying sand layer Figure 5-5 and Figure 5-6). In addition, there were flames extending upward from this sand layer into overlying silt layers. Organic samples RnR1-C1 and RnR1-C2 were collected 3.55 m and 3.08 m BS, respectively. RnR1-C2 was collected near the top of the interbedded silt and sand deposit in which the SSDs formed. RnR1-C1 was collected from an underlying deposit of mottled, very fine sandy silt. RnR1-C2 yielded calibrated ages of 43-Post 0, 118-60, 230-135, and 290-250 yr B.P. with a 76% probability that the SSDs formed before 60 yr B.P. or A.D. 1890 (Table D-1). RnR1-C1 yielded calibrated ages of 1830-1702 and 1652-1644 yr B.P., with a 94.3 probability for the earlier range. The SSDs likely formed between 1830-60 yr B.P., and probably closer in age to 60 yr B.P. since RnR1-C2 came from the interbedded silt and sand deposit. What may be the remnants of an historical corduroy road was found in the cutbank about 40 m north of RnR1. Therefore, the site and adjacent cutbanks warrants additional study to determine whether or not construction of the corduroy road might have contributed to deformation at the site. If not, it would be worthwhile to collect additional samples, including sediment samples for OSL dating, to further constrain the timing of deformation.

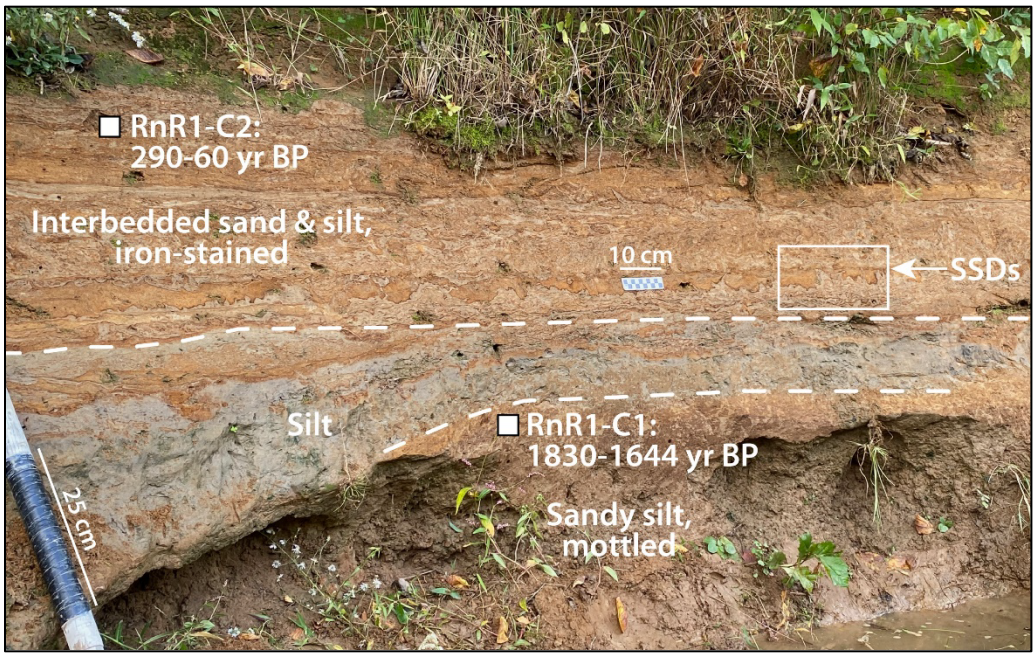

Figure 5-5: **Photograph of lower 1.5 m of bank at site RnR1 showing iron-stained interbedded sand and silt underlain by gray silt followed by mottled, sandy silt. SSDs occurred within iron-stained interbedded sand and silt. C14 dating of samples RnR1-C2 and RnR1-C1, collected above and below the SSDs, respectively, indicates that the deformation structures formed between 1830-60 yr B.P. White rectangle outlines area of closeup of SSDs shown in Figure 5-6.**

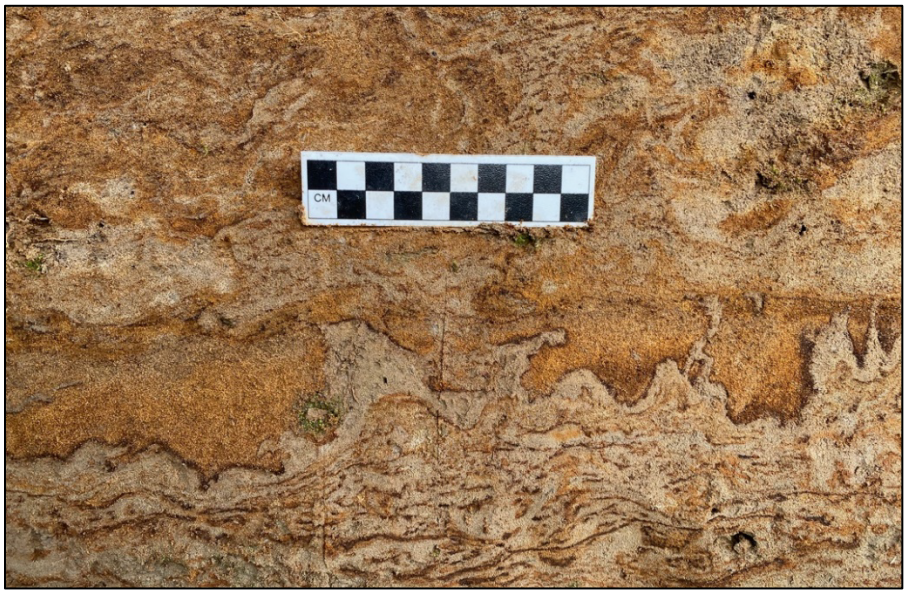

Figure 5-6: **Closeup of SSDs at site RnR1 showing pseudonodules or rounded masses of iron-stained sand sinking downward into silty sand layer below and diapirs of silty sand extending upward into overlying sand layer. Both layers may have liquefied and mobilized, leading to the formation of the SSDs.**

At site RnR3, a sand dike, 1 cm wide at the base of the cutbank, extended 25 cm into the overlying mottled silt and branched upward before becoming difficult to trace due to bioturbation. The dike was planar suggesting that it is an earthquake-induced liquefaction feature and not a tree root cast. At the same level as and within 0.75 m of the upper part of the dike, there were a couple of sandy domains, 2-3 cm wide, in the mottled silt that could be related to the dike. In addition, a small flame structure, which verged upstream, extended upward from a thin layer of sand into the overlying silt. These small features suggest that earthquake-induced liquefaction occurred at the site. Probing below the water level, interbedded silt and sand continued for only 0.5 m where bedrock was encountered. Unfortunately, no organic samples were found at this site for C14 dating.

The type of SSDs observed at RnR1 and RnR3 may be the result of earthquake-induced liquefaction (Sims, 1975, 2012; Tuttle et al., 2019a). The combination of SSDs, including a small sand dike at RnR3, supports an earthquake origin. Sedimentary conditions along the river are not ideal for the formation of liquefaction features. Many of the sand layers are thin, limiting the amount of water and sediment that can be mobilized to form features. Perhaps these conditions led to the formation of pseudonodules and diapirs, rather than sand dikes. Also, the sediment section is very thin ($\leq$6 m) and likely fairly young, as suggested by the maximum age of 1830 yr B.P. for RnR1-Cl, thus limiting the potential liquefaction record of earthquakes to the past 2 kyr.

If the SSDs at RnR1 and RnR3 formed as a result of liquefaction, they may have been caused by an historical earthquake, though a prehistorical earthquake is also possible. SSDs such as those at RnR1 and RnR3 have been attributed to earthquakes of **M** 5 or larger by Uner (2014) and Modified Mercalli intensities as low as VIII by Sims (1973).

5.5 Appomattox River

Along the Appomattox River, the survey for liquefaction features was conducted south of Macon from a location west of the Rt. 609 bridge downstream for 8 km to Rocky Ford Creek. Along this stretch of the river, the modern flood plain ranges from 0.3-0.5 km wide. In a few places, the river flows along the edge of the flood plain adjacent to steep banks with rock outcrops. Holocene and upper Pleistocene alluvium of sand, silt, and clay underlie the modern flood plain which was 3-4 m above the river at the time of the survey (Table B-1). Also, cutbank exposures occurred in most river bends (Table 5-1). Though the upper 0.5-2 m were mostly covered with vegetation, the lower 1-2.3 m of the banks usually revealed silty sand underlain by mottled silt followed by mottled silty sand or sandy silt. Occasionally, pebbles and cobbles occurred within the silty sand near the base of the cutbank. Probing up to 1.6 m below the water level, silt, sandy silt, silty sand, and sand were encountered, with sand often becoming more common and coarser with depth.

At sites AR5 and AR6, silty, very fine sand with a small component of coarse sand appeared to have been injected into cracks within mottled, yellowish-red, very fine sandy silt (Table C-1). At both sites, the sand dikes, up to 10 cm wide, narrowed and branched upward, were bioturbated and mottled, and extended 0.6 m above the river level where they became difficult to trace. At AR7, a 12-cm-wide sand dike exposed near the base of the cutbank gave rise to two smaller dikes and a diapir (Figure 5-7). One of the dikes extended to 50 cm above the river level where sand accumulated below a rock fragment, wrapped around the fragment, and pinched out 65 cm above the river level. This phenomenon of sand accumulation below obstacles encountered during injection of dikes was observed in Ferland, Quebec, where sand dikes and related sand blows formed during the 1988 **M** 5.9 Saguenay earthquake (Tuttle et al., 1990).

At site AR8, there appeared to be two generations of liquefaction features (Figure 5-8; Table C-1). The older generation of features includes silty sand injected through krotovinas (filled-in animal burrows) lower in the cutbank and sand dikes higher in the section. The sand dikes, up to 10 cm wide, narrowed and branched upward, were iron stained, mottled, and bioturbated especially along their margins. Some of the dikes were connected to a sand sill that formed at the base of a very weathered silt layer containing many large manganese nodules. Other dikes terminated at this boundary while others branched into smaller dikes and continued upward. Some of the dikes extended to 2.25 m above the river level or 1.55 m below the top of the cutbank. None of the sand dikes crosscut the boundary between silt loam and an overlying, less weathered, silty sand deposit. The younger generation of features were unweathered, relatively small, 1-2 cm wide, silty, medium to fine sand dikes that crosscut the lower portion of the cutbank and the previously injected krotovinas. These dikes were also visible crosscutting sediment below the water level.

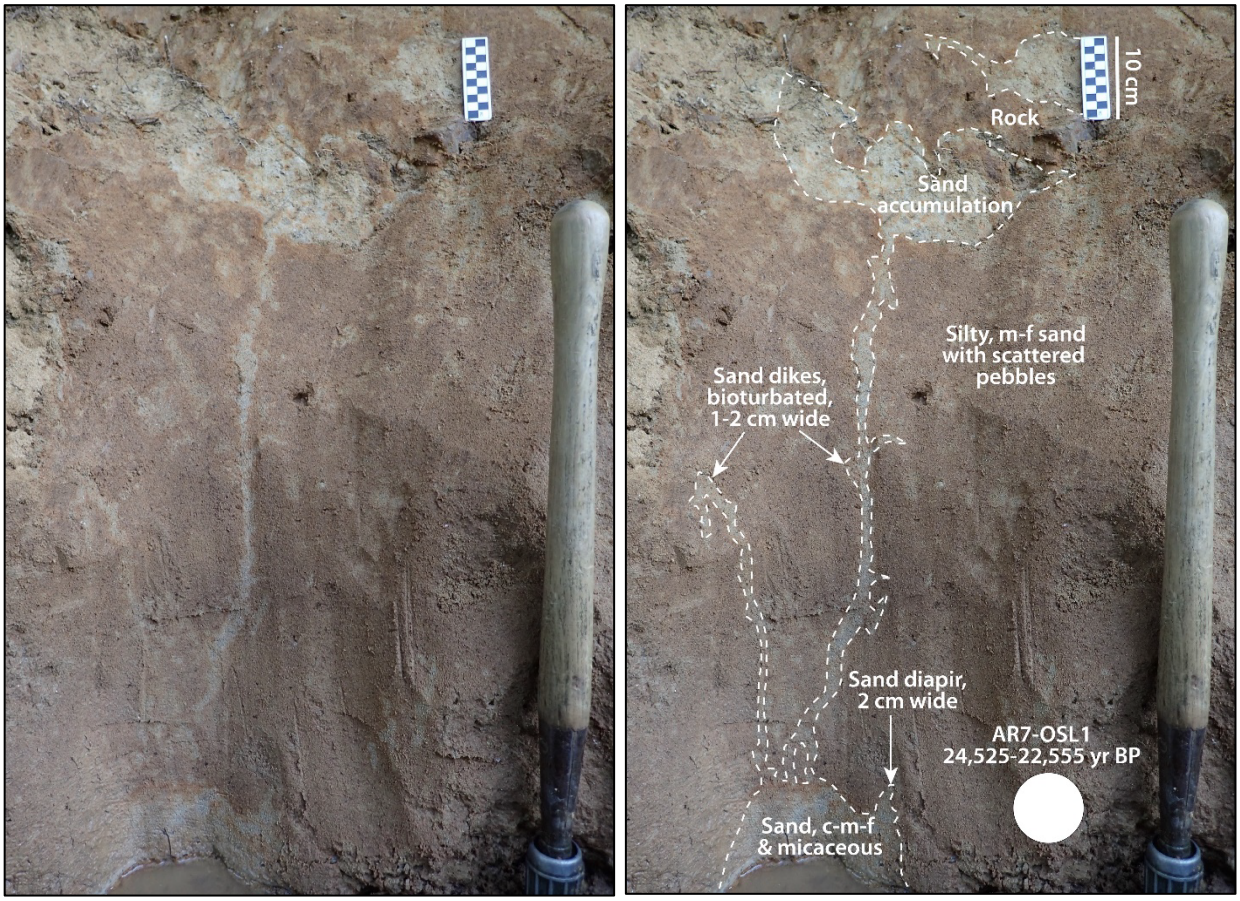

Figure 5-7: Photographs (left unannotated; right annotated) of sand dikes and diapir exposed in lower 70 cm of cutbank at site AR7 along the Appomattox River. Probing detected silty sand to 1.1 m followed by sand to 1.5 m below the water level. Black and white squares of small scale represent centimeters and shovel handle is 50 cm long.

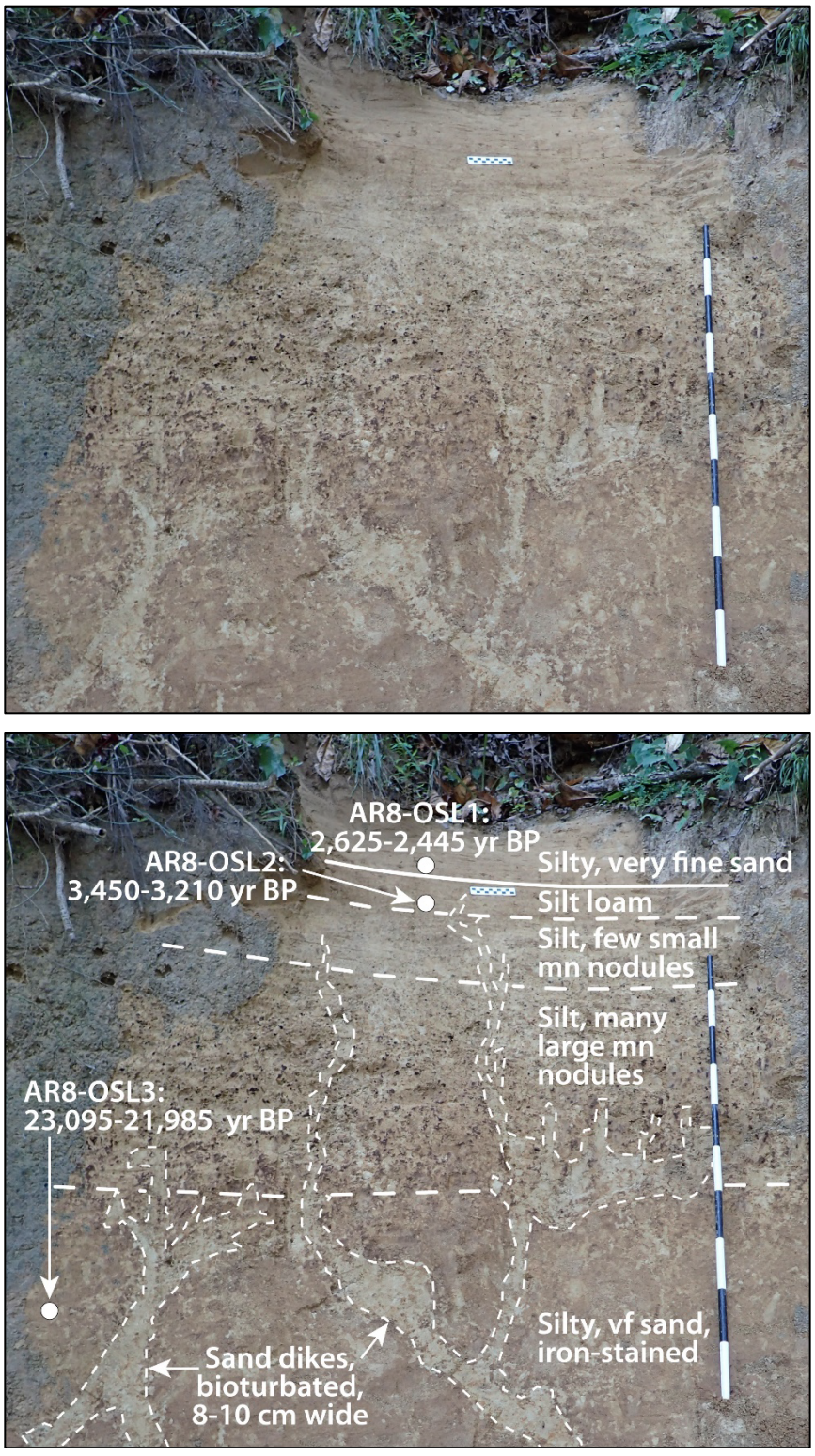

Figure 5-8: **Photographs (upper unannotated; lower annotated) of sand dikes exposed in cutbank at site AR8 along the Appomattox River. Probing detected silty sand to 0.82 m, sand to 0.94 m, followed by silty sand to 1.5 m below the water level. Black and white intervals of the meter stick represent decimeters and squares of the small scale represent centimeters.**

At both sites AR5 and AR7, sediment samples were collected about 2.9 m below the top of the cutbank or 10 cm above the base of the cutbank for OSL dating (Figure 5-7; Table D-2). They yielded overlapping OSL ages of 27,520-23,140 yr B.P. and 24,525-22,555 yr B.P. for AR5 and AR7, respectively. At AR8, a suite of three sediment samples was collected 1.45 m BS near the bottom of the upper unit of silty sand, 1.59 m BS from the sandy silt below the silt loam horizon at the top of the lower unit, and 2.39 m BS from the silty fine sand from the lower unit (Figure 5-8). From positions higher to lower in the cutbank, the samples yielded OSL ages of 2,625-2,445 yr B.P., 3,450-3,210 yr B.P., and 23,095-21,985 yr B.P. (Table D-2). The results suggest that the sediment exposed in the 3-4 m high cutbanks along this portion of the Appomattox River was deposited during the upper Pleistocene and Holocene and that the older liquefaction features formed between 2,450-3,450 yr B.P.

As mentioned in Section 4.2, sedimentary conditions are nearly ideal for the formation of earthquake-induced liquefaction features along this stretch of the Appomattox River. The liquefaction features found along the Appomattox suggest two earthquakes during the past 3.5 kyr. This is similar to findings of previous paleoliquefaction studies in the CVSZ (Tuttle et al., 2021). Also, the dating of the older generation of liquefaction features at AR8 helps to constrain the timing of the prehistorical earthquake that struck this area to 3 ka ± 500 yr.

6 EARTHQUAKE-INDUCED LIQUEFACTION AND EVENT TIMING

The most significant findings during the river surveys are likely earthquake-induced liquefaction features along the Appomattox River southwest of Richmond and possible liquefaction features along the Rapidan River west of Fredericksburg (Table 6-1). The features along the Appomattox include an older generation of weathered sand dikes and intruded krotovinas and a younger generation of unweathered sand dikes that crosscut the older generation of features. On the basis of OSL dating, the older Appomattox features formed between 3450-2450 yr B.P.

The age of the older generation of liquefaction features along the Appomattox River overlaps with that estimated ages for liquefaction features previously found along the Mattaponi and Pamunkey Rivers. The ages of features on the Mattaponi and Pamunkey Rivers were poorly constrained between 280 and 2730 yr B.P. based on maximum constraining ages and weathering characteristics (Tuttle et al., 2021). There are other features along these two rivers and the Rivanna and South Anna Rivers that may have formed during the same Late Holocene earthquake but their maximum constraining ages allow for an earlier time(s) of formation. Although not required, it seems likely that the weathered features along the Appomattox, Mattaponi, Pamunkey, Rivanna, and South Anna Rivers formed as the result of the same earthquake given their similarity in weathering characteristics and the absence of cross-cutting relationships. If so, dating of the features on the Appomattox River helps to narrow the age estimate of the Late Holocene earthquake to 3 ka ± 500 yr (Table 6-1). Also, the finding of liquefaction features along the Appomattox River extends the area of liquefaction for this event farther south. The average size of the older sand dikes along the Appomattox River is larger than sand dikes along any of the other rivers, suggesting that the paleoearthquake may have been located closer to the Appomattox or possibly between the Appomattox and the Mattaponi Rivers.

The unweathered sand dikes along the Appomattox River, similar to unweathered sand dikes previously found along the James River, probably formed during one of the historical earthquakes, most likely the 1758, 1774, or 1875 event.

Table 6-1: Summary of Earthquake-Induced Liquefaction Features, Age Information, and Event Timing

River Name	Liquefaction Features	Dike Width (cm)	Average Dike Width (cm)	Weathering	Age Constraint* Yr B.P. (1950)	Event Timing
Appomattox	Sand dikes & intruded krotovinas	2 0.5-12	2 5.5	Unweathered & weathered	NA 3450-2450	Historical & 3 ka ± 500 yr
Rapidan	Sand dike & SSDs	1	1	Gleyed Iron stained	1830-60	Historical or prehistorical < 1.9 ka

* Calibrated C14 ages and OSL ages rounded to the nearest 10 years. NA - not applicable.

Features of interest found along the Rapidan River include one small sand dike and SSDs, more specifically, pseudonodules, diapirs, and flames. Although these SSDs can form as the result of sedimentary processes, the presence of the sand dike suggests that they formed as the results of earthquake-induced liquefaction. On the basis of C14 dating, the Rapidan features formed between 1830-60 yr B.P.

Therefore, the features may have formed during an historical earthquake, most likely the 1758 event given its estimated size and location, or alternatively during a prehistorical earthquake

sometime since 1830 yr B.P. (Table 6-1). If the later were the case, it would indicate a previously unrecognized paleoearthquake near the northern margin of the CVSZ. Additional study and dating of possible liquefaction features at sites along the river would help to further evaluate if they formed during an historical or prehistorical earthquake during the past 1.9 kyr.

No historical or prehistorical liquefaction features were found along the Mattaponi, Rappahannock, or Potomac Rivers or its adjoining estuaries of Popes, Rosier, and Upper Machodoc Creeks. Along the 15 km of the Mattaponi River downstream from the Rt. 628 bridge near Beulahville, sedimentary conditions were adequate for liquefaction features to have formed in Late Holocene alluvium during historical earthquakes and in upper Pleistocene alluvium during historical and prehistorical earthquakes so long as the sediment was saturated at the time of the earthquakes. In addition, exposure of Late Holocene and upper Pleistocene alluvium was adequate to have found liquefaction features, if they had formed. Therefore, the absence of liquefaction features along the 15 km downstream from the Rt. 628 bridge suggests that ground shaking was not strong enough in this area to induce liquefaction during historical earthquakes or the paleoearthquake ~3 ka. Assuming this interpretation is true, it helps to define the eastern limit of liquefaction for this event.

Along the Rappahannock River, exposure of Holocene and upper Pleistocene alluvium is poor. In addition, most sediment suitable for the formation of liquefaction features is too young to record earthquake-induced liquefaction more than 150 yr ago or prior to A.D. 1850. Along the Potomac River or its adjoining estuaries, there is very little exposure of Holocene alluvium; exposure of upper Pleistocene alluvium is much better but sedimentary conditions are not suitable for the formation of liquefaction features. Therefore, the absence of earthquake-induced liquefaction features along the Rappahannock River and the Potomac River or its adjoining estuaries is not particularly meaningful in regard to past earthquakes.

7 EVALUATION OF LOCATIONS AND MAGNITUDES OF EARTHQUAKES

Building on previous research, scenario earthquakes are further evaluated that could account for the features along the Appomattox and Rapidan Rivers found during this study. Along the Appomattox, likely liquefaction features include unweathered sand dikes thought to have formed during an historical earthquake and weathered sand dikes and intruded krotovinas that probably formed during a paleoearthquake ~3 ka ± 500 yr. In this evaluation, all of the prehistorical features including those previously found along the Mattaponi, Pamunkey, Rivanna, and South Anna Rivers are assumed to have formed during the same paleoearthquake. Along the Rapidan River, possible liquefaction features include pseudonodules, diapirs, flames, and one sand dike that formed since 1830 yr B.P.

On the basis of the relation between earthquake magnitude and distance to farthest liquefaction features in very susceptible sediment (Ambraseys, 1988; Castilla and Audemard, 2007), historical liquefaction features on the Appomattox, James, and Pamunkey Rivers could have formed during three **M** ≥ 5.0 earthquakes so long as the earthquakes occurred within 18 km of each group of liquefaction features Figure E-1a and Table 7-1). Alternatively, the features could have formed during one earthquake if it were of **M** ≥ 5.5 and located between and within 29 km of the three groups of features. On the basis of liquefaction potential analysis (e.g., Seed and Idriss, 1971 and 1982; Youd et al., 2001; Cetin et al., 2004; Idriss and Boulanger, 2004; Green et al., 2005; Tuttle et al., 2019a) which utilizes borehole data in the vicinity of liquefaction features, the historical liquefaction features along the three rivers could have formed as the result of three **M** 5.25-5.5 earthquakes if they were located within 10 km of the features or as the result of one **M** ≥ 6.0 earthquake if it were located between and within 30 km of the features (Table E-2 and Table 7-1). Magnitude estimates based on the magnitude-distance relation are likely to represent minimum values; whereas, slightly higher estimates based on liquefaction potential analysis may be more realistic given the predominantly loose (N values 4-10) soil conditions of sandy sediment along the three rivers.

It seems very unlikely that one **M** ≥ 6.0 earthquake was responsible for the historical liquefaction features on the Appomattox, James, and Pamunkey Rivers given that none of the pre-instrumental earthquakes were estimated to be greater than **M** 5.32 (Table A-1 and Figure A-1). It seems much more likely that the historical liquefaction features were caused by the 1758, 1774, and 1875 earthquakes and that these events may have been slightly larger, **M** 5.0-5.5, than previously estimated.

Table 7-1: Summary of Magnitude Estimates for Historical and Prehistorical Earthquakes

Earthquake	Previous Results (Tuttle et al., 2021)		Magnitude-Distance Relation*		Liquefaction Potential Analysis*	
	1 Event	2 Events	1 Event	3 Events	1 Event	3 Events
Historical	**M** 5.75	**M** 5.0-5.25	**M** ≥ 5.5	**M** ≥ 5.0	**M** ≥ 6.0	**M** 5.25-5.5
Prehistorical ~3 ka	**M** 6.25-6.5	**M** 6.0 & **M** 6.25	**M** ≥ 6.1, **M** ≥ 6.4, or **M** ≥ 6.6	**M** ≥ 5.5-5.7	**M** 6.5-6.75	**M** 6.25-6.5

*Preferred magnitude estimates are shaded gray.

For prehistorical features, scenario earthquakes are further evaluated for possible source areas near (1) the 2011 Mineral, VA, earthquake, (2) Holly Grove in the middle of the distribution of

liquefaction features, and (3) Ashland, where a cluster of small earthquakes have been recorded since 1974 and previously noted during studies of the CVSZ. On the basis of the magnitude-distance relation of Castilla and Audemard (2007), the prehistorical features could have formed during one earthquake if it were of **M** $\geq$ 6.1 and located near Holly Grove, **M** $\geq$ 6.4 and located near Mineral, or **M** $\geq$ 6.6 and located near Ashland or Appomattox (Figure E-1b, dark gray shading; and Table 7-1). Alternatively, the prehistorical features could have formed during three **M** $\geq$ 5.5-5.7 earthquakes located in the Ashland, Mineral, and Appomattox areas (Figure E-1b, light gray shading). According to liquefaction potential analysis, all the prehistorical features could have formed during one earthquake if it were of **M** 6.5-6.75 and located near Holly Grove or **M** 6.75 -7.0 and located near either Mineral or Ashland (Table E-3, Table E-4, and Table E-5). Alternatively, the features could have formed during three **M** 6.25-6.5 earthquakes centered near Mineral, Holly Grove, and Ashland (Table 7-1). The liquefaction features along the Appomattox River are located west of the Fall Line; therefore, their relatively large size is not related to amplification of ground motion by Coastal Plain sediment as was suggested for the larger sand dikes along the Pamunkey and Mattaponi Rivers.

Given their similarity in weathering characteristics and lack of cross-cutting relationships with one another, the prehistorical liquefaction features may have formed during one large earthquake. Also, considering the size distribution of liquefaction features, the paleoearthquake may have been located between the Appomattox and Mattaponi Rivers. Therefore, an earthquake of **M** 6.5-6.75 located near Holly Grove is preferred, though other locations between the Appomattox and Mattaponi Rivers are also possible (Table 7-1).

As mentioned in Section 6, possible earthquake-induced liquefaction features found along the Rapidan River may have formed during an historical earthquake. The March 23, 1758, earthquake of **M** 4.95 $\pm$ 0.371 has an assigned epicentral location near Luther Glen with a horizontal error of 50 km (Table A-1 and Figure A-1). Therefore, the 1758 earthquake may have been of **M** 5.32 and located within 21 km of the Rapidan River sites. According to the magnitude-distance relation, a **M** 5.3 earthquake can induce liquefaction up to 24 km from its epicenter (Figure E-1), suggesting the 1758 earthquake could have been responsible for the Rapidan features. However, liquefaction potential analysis indicates that an earthquake of **M** 5.5-5.75 located within 10 km or **M** 6.0 located within 20 km would be required to induce liquefaction along the Rapidan (Table E-1 and Table E-2). This suggests that either the 1758 earthquake was not responsible for the features along the Rapidan or that the 1758 earthquake was larger and located farther west than previously estimated.

8 CONCLUSIONS

During this study, features likely to be earthquake-induced liquefaction features were found in Holocene and upper Pleistocene alluvium along the Appomattox River southwest of Richmond. In addition, features that might be earthquake-induced liquefaction features were found in Late Holocene alluvium along the Rapidan River west of Fredericksburg. The Appomattox features include a younger generation of unweathered sand dikes and an older generation of weathered sand dikes and intruded krotovinas. The younger generation of features likely formed during an historical earthquake, and the older generation of features probably formed during a paleoearthquake ~3 ka ± 500 yr. The Rapidan features include pseudonodules, diapirs, flames, and a sand dike that probably formed between 1830-60 yr B.P. during either an historical earthquake or a previously unrecognized paleoearthquake near the northern margin of the CVSZ.

Although Holocene and upper Pleistocene alluvium were present and exposed, no earthquake-induced liquefaction feature was found along the Mattaponi River for 15 km downstream from the Rt. 628 bridge near Beulahville, suggesting that ground motion was not strong enough to induce liquefaction in this area during historical earthquakes or the paleoearthquake ~3 ka. In contrast, there was very little exposure of Holocene and upper Pleistocene alluvium along the Rappahannock and Potomac Rivers or the estuaries of Popes, Rosier, and Upper Machodoc Creeks. What little Holocene alluvium was exposed along the Rappahannock River appears to be too young to have recorded events prior to 100 yr B.P. or A.D. 1850.

The historical liquefaction features along the Appomattox, James, and Pamunkey Rivers are interpreted to have formed as result of three **M** 5.0-5.5 earthquakes located in close proximity to the three groups of features. Of known pre-instrumental earthquakes, the 1758, 1774, and 1875 events seem to be the most likely to have induced liquefaction along the three rivers. If so, they may have been slightly larger than previously estimated. The prehistorical liquefaction features along the Appomattox, Mattaponi, Pamunkey, Rivanna, and South Anna Rivers are interpreted to have formed ~3 ka ± 500 yr during one **M** 6.5-6.75 earthquake centered near Holly Grove or farther east between the Appomattox and Mattaponi Rivers.

Uncertainties remain regarding the origin and age of some of the features, as well as the extent of liquefaction, especially along the Appomattox River in the southern part of the CVSZ. Additional survey for, study and dating of, likely liquefaction features would help to reduce these uncertainties and to test the interpretations that (1) a **M** 6.5-6.75 earthquake struck the region ~3 ka ± 500 yr causing liquefaction in susceptible sediment across the region, (2) several historical earthquakes were large enough, **M** 5.0-5.5, to induce liquefaction locally, and (3) either an historical or prehistorical earthquake induced liquefaction near the northern margin of the CVSZ during the past 1.9 kyr.

9 REFERENCES

Ambraseys, N N., 1988, Engineering seismology: earthquake engineering and structural dynamics, Journal of the International Association of Earthquake Engineering, v. 17, p. 1-105.

Atkinson, G., and Boore, D., 2011, Modification to existing ground-motion prediction equations in light of new data, Bulletin of the Seismological Society of America, v. 101, n. 3, p. 1121- 1135.

Atkinson, G., (with input from) J. Adams, G. Rogers, T. Onur, and K. Assatourians, 2012, White paper on development of ground motion prediction equations for Canadian national seismic hazard maps, www.seismotoolbox.ca (Miscellaneous Resources).

Atkinson, G., (Project Leader), K. Assatourians, 2012, GMPEs for national hazard maps, www.seismotoolbox.ca (Miscellaneous resources).

Bronk Ramsey, C., 2009, Bayesian analysis of radiocarbon dates, Radiocarbon, v. 51, n. 1, p. 337-360.

Building Seismic Safety Council, 1997, NEHRP recommended provisions for seismic regulations for new buildings and other structures, FEMA 302, Part 1 Provisions, Prepared for the Federal Emergency Management Agency, Washington, D.C.

Carter, M.W., 2015, Characterizing pedogenic and potential paleoseismic features in South Anna River alluvium: epicentral region of the 2011 earthquake Central Virginia seismic zone, Presentation at the 2015 Virginia Geological Research Symposium.

Castilla, R.A.; Audemard, F.A., 2007, Sand blows as a potential tool for magnitude estimation of pre-instrumental earthquakes, Journal of Seismology, v. 11, p. 473–487. doi:10.1007/s10950-007-9065-z.

Cetin, K.O., Seed, R.B., Der Kiureghian, A., Tokimatsu, K., Harder, L.F. Jr, Kayen, R.E., Moss, R.E.S., 2004, SPT-based probabilistic and deterministic assessment of seismic soil liquefaction potential, ASCE Journal of Geotechnical and Environmental Engineering, v. 130, n. 12, p. 1314-1340.

Chapman, M.C., 2013, On the rupture process of the 23 August 2011Virginia earthquake, Bulletin of the Seismological Society of America, v. 103, p. 613-628.

Chapman, M.C., 2015, Magnitude, recurrence interval, and near-source ground motion modeling of the Mineral, Virginia, earthquake of 23 August 2011, *in* Horton, J. W., Jr., Chapman, M. C., and Green, R. A., eds., The 2011 Mineral, Virginia, earthquake, and its significance for seismic hazards in eastern North America, Geological Society of America Special Paper 509, p. 27-45.

Cohen, K.M., S.C. Finney, P.L. Gibbard, and J.-X. Fan, updated 2022, The ICS International Chronostratigraphic Chart, Episodes 36, p. 199-204, http://www.stratigraphy.org/ICSchart/ChronostratChart2022-10.pdf

Dicken, C.L., Nicholson, S.W., Horton, J.D., Kinney, S.A., Gunther, G., Foose, M.P., Mueller, and J.A.L., 2008, Preliminary integrated geologic map databases for the United States: Delaware, Maryland, New York, Pennsylvania, and Virginia, U.S. Geological Survey, Open-File Report 2005-1325, https://pubs.usgs.gov/of/2005/1325/

Dobry, R., R.D. Borcherdt, C.B. Crouse, I.M. Idriss, et al., 2000, New site coefficients and site classification system used in recent building seismic code provisions, Earthquake Spectra, v. 16, p. 44-67.

Dominion, 2004, Response to request for additional information no. 3, North Anna Early Site Permit Application, Dominion Nuclear North Anna, LLC, U.S. Nuclear Regulatory Commission, Report ML042800292, 110 p.

Ebel, J. E., Bonjer, K., and Oncescu, M., 2000, Paleoseismicity: seismicity evidence for past large earthquakes, Seismological Research Letter, v. 71, p. 283-294. doi:10.1785/gssrl.71.2.283

Electric Power Research Institute (EPRI), US Department of Energy (DOE), and US Nuclear Regulatory Commission (NRC), 2012, Central and Eastern United States Seismic Source Characterization for Nuclear Facilities, NUREG-2115, EPRI, Palo Alto, CA.

Green, R.A., Obermeier, S.F., Olson, S.M., 2005, Engineering geologic and geotechnical analysis of paleoseismic shaking using liquefaction effects: field examples, Engineering Geology, v. 76, p. 263-293.

Green, R., Lasley, S., Carter, M.W., Munsey, J.W., Maurer, B W., Tuttle, M.P., 2015, Geotechnical aspects in the epicentral region of the 2011 Mw 5.8 Mineral, Virginia, earthquake, in Horton, J.W., Jr., Chapman, M.C., and Green, R.A., eds., The 2011 Mineral, Virginia, earthquake, and its significance for seismic hazards in eastern North America, Geological Society of America Special Paper 509. doi:10.1130/2015.2509(09)

Horton, J.W., Chapman, M.C., and Green, R.A., 2015, The 2011 Mineral, Virginia, earthquake, and its significance for seismic hazards in eastern North America-Overview and synthesis, *in* Horton, J. W., Jr., Chapman, M. C., and Green, R. A., eds., The 2011 Mineral, Virginia, earthquake, and its significance for seismic hazards in eastern North America, Geological Society of America Special Paper 509, p. 1-25.

Hough, S.E., 2012, Initial assessment of the intensity distribution of the 2011 Mw5.8 Mineral, Virginia, earthquake, Seismological Research Letters, v. 83, 649–657. https://doi.org/10.1785/0220110140

Hughes, K.S., Hibbard, J.P., and Bohnenstiehl, D.R., 2015, Relict Paleozoic faults in the epicentral area of the August 23, 2011 central Virginia earthquake: Assessing the relationship between preexisting strain and modern seismicity, *in* Horton, J.W., Jr., Chapman, M.C., and Green, R.A., eds., The 2011 Mineral, Virginia, earthquake, and its significance for seismic hazards in eastern North America, Geological Society of America Special Paper 509, p. 331- 343.

Idriss, I.M., and Boulanger, R.W., 2004, Semi-empirical procedures for evaluating liquefaction potential during earthquakes, Proc., 11th International Conference on Soil Dynamics and Earthquake Engineering, and 3rd International Conference on Earthquake Geotechnical Engineering, D. Doolin et al., eds., Stallion Press, v. 1, p. 32-56.

Juang, C.H., and Jiang, T., 2000, Assessing probabilistic methods for liquefaction potential evaluation, Soil Dynamics and Liquefaction 2000, GSP 107 (Proceedings GeoDenver), American Society of Civil Engineers, Reston, VA.

Kempthorne, D., and Myers, M.D., 2006, The Virginia Coastal Plain hydrogeologic framework, U.S. Geological Survey, Professional Paper 1731, 114 p.

Liang, P., and Forman, S.L., 2019, LDAC: An Excel-based program for luminescence equivalent dose and burial age calculations, Ancient TL, v. 37, p. 21-40.

Malenda, H.F., Raup, C., Pazzaglia, F.J., and Berti, C., 2014, Surficial geologic map of the South Anna River in the Ferncliff and Pendleton quadrangles, Virginia. U.S. Geological Survey, EDMAP, Open File Map G13AC0015; scale 1:24,000.

Mixon, R.B., Berquist, C.R., Jr., Newell, W.L., and Johnson, G.H., 1989, Geological map and generalized cross section of the Coastal Plain and adjacent parts of the Piedmont, Virginia, U.S. Geological Survey, Miscellaneous Investigations Series Map I-2033; scale 1:250,000.

Mixon, R.B., Pavlides, L., Powars, D.S., Froelich, A.J., et al., 2000, Geological map of the Fredericksburg 30' x 60' quadrangle, Virginia and Maryland, U.S. Geological Survey, Geological Investigations Series Map I-2607; scale 1:100,000.

Mueller, C.S., 2019, Earthquake catalogs for the USGS National Seismic Hazard maps, Seismological Research Letters, v. 90, n. 1, p. 251-261. https://doi.org/10.1785/0220170108

Newell, W.L., Bricker, O.P., and Robertson, M.S., 2006, Geologic map of the Colonial Beach South 7.5' Virginia quadrangle, U.S. Geological Survey, Open File-2005-1025; scale 1:24,000.

Obermeier, S.F., 1996, Using liquefaction-induced features for paleoseismic analysis, *in* McCalpin, J. P., ed., Paleoseismology, Academic Press, San Diego, CA, p. 331-396.

Obermeier, S.F., and McNulty, W.E., 1998, Paleoliquefaction evidence for seismic quiescence in central Virginia during late and middle Holocene time, EOS, Transactions of the American Geophysical Union, v. 79, no. 17, Spring Meeting Supplement, Abstract T41A-9.

Pazzaglia, F.J. Carter, M.W., Berti, C., Counts, R., Hancock, G., Harbor, D., Harrison, R., Heller, M., Mahan, S., Malenda, H., McKeon, R., Nelson, M., Prince, P., Rittenour, T., Spotila, J., and Whittecar, R., 2015, Geomorphology, active tectonics, and landscape evolution in the Mid-Atlantic region, *in* Brezinski, D.K., Halka, J.P., and Ortt, R.A., Jr., eds., Tripping from the Fall Line: Field Excursions for the GSA Annual Meeting, Baltimore, 2015: Geological Society of Field Guide 40, p. 109–169. doi:10.1130/2015.0040(06)

Pazzaglia, F.J., Malenda, H.F., McGavick, M.L., Raup, C., Carter, M.W., Berti, C., Mahan, S., Nelson, M., Rittenour, T.M., Counts, R., Willenbring, J., Germanoski, D., Peters, S.C., and Holt, W.D., 2021, River terrace evidence of tectonic processes in the eastern North American Plate interior, South Anna River, Virginia: The Journal of Geology, v. 129, n. 5, University of Chicago. https://doi.org/10.1086/712636

Petersen, M.D., Frankel, A.D., Harmsen, S.C., Mueller, C.S., Haller, K.M., Wheeler, R.L., Wesson, R.L., Zeng, Y., Boyd, O.S., Perkins, D.M., Luco, N., Field, E.H., Wills, C.J., and Rukstales, K.S., 2008, Documentation for the 2008 update of the United States National Seismic Hazard Maps, U.S. Geological Survey Open-File Report 2008-1128, 61 p.

Powars, D.S., Catchings, R.D., Horton, J.W., Jr., Schindler, S., and Pavich, M.J., 2015, Stafford fault system: 120 million year fault movement history of northern Virginia, *in* Horton, J.W., Jr., Chapman, M.C., and Green, R A., eds., The 2011 Mineral, Virginia, earthquake, and its significance for seismic hazards in eastern North America, Geological Society of America Special Paper 509, p. 407-431.

Pratt, T.L., Horton, J.W, Jr., Muñoz, J., Hough, S.E., Chapman, M.C., and Olgun, C.G., 2017, Amplification of earthquake ground motions in Washington, D.C., and implications for hazard assessments in central and eastern North America, Geophysical Research Letters, v. 44. https://doi.org/10.1002/2017GL075517

Prescott, J.R., and Hutton, J.T., 1994, Cosmic ray contributions to dose rates for luminescence and ESR dating: Large depths and long-term time variations, Radiation Measurements, v. 23, p. 497-500.

Reimer, P.J., Austin, W E.N., Bard, E., Bayliss, A., et al., 2020, The IntCal20 northern hemisphere radiocarbon age calibration curve (0-55 cal kBP), Radiocarbon, v. 62, n. 4, p. 725-757. doi: 10.1017/RDC.2020.41

Rukstales, K.S., and Petersen, M.D., 2019, Data release for 2018 update of the U.S. National Seismic Hazard Model: U.S. Geological Survey data release, https://doi.org/10.5066/P9WT5OVB

Schindler, J.S., Harrison, R.W., and Obermeier, S.F., 2012, Review and update of paleoliquefaction evidence for Holocene seismic activity in the CVSZ, [abs.] Eastern Section, Seismological Society of America, Program and Abstracts, p. 43.

Seed, H.B. and Idriss, I.M., 1971, Simplified procedure for evaluating soil liquefaction potential. Journal of the Soil Mechanics & Foundations Division (ASCE), v. 97 (SM9), p. 1249-1273.

Seed, H.B., and Idriss, I.M., 1982, Ground motions and soil liquefaction during earthquakes, Earthquake Engineering Research Institute, Berkley, 134 p.

Sims, J.D., 1973, Earthquake-induced structures in sediments of Van Norman Lake, San Fernando California, Science, v. 182, p. 161-163.

Sims, J.D., 1975, Determining earthquake recurrence intervals from deformational structures in young lacustrine sediments, Tectonophysics, v. 29, p. 141–153. doi:10.1016/0040-1951(75)90139-0

Sims, J.D, 2012, Earthquake-induced load casts, pseudonodules, ball-and-pillow, and convolute lamination: additional deformation structures for paleoseismic studies, *in* Cox, R.T., Tuttle, M.P., Boyd, O.S., Locat, J., eds., Recent advances in North American paleoseismology and neotectonics east of the Rockies, Geological Society of America, Special Paper 493, p. 191–202. doi:10.1130/2012.2493(09)

Tuttle, M., Law, T., Seeber, L., and Jacob, K., 1990, Liquefaction and ground failure in Ferland, Quebec, triggered by the 1988 Saguenay Earthquake, Canadian Geotechnical Journal, v. 27, p. 580-589.

Tuttle, M.P., 2001, The use of liquefaction features in paleoseismology: Lessons learned in the New Madrid seismic zone, central United States, Journal of Seismology, v. *5*, p. 361-380.

Tuttle, M.P., and Hartleb R., 2012, Appendix E. Central and Eastern U.S. paleoliquefaction database, uncertainties associated with paleoliquefaction data, and guidance for seismic source characterization, *in* The Central and Eastern U.S. Seismic Source Characterization for Nuclear Facilities, Technical Report, EPRI, Palo Alto, CA, U.S. DOE, and U.S. NRC, 135 p. plus database.

Tuttle, M.P., Villamor, P. Almond, P., et al., 2017, Liquefaction induced during the 2010-2011 Canterbury, New Zealand, earthquake sequence and lessons learned for the study of paleoliquefaction features, Seismological Research Letters, v. 88, p. 1403-1414, plus supplement. doi:10.1785/0220170073

Tuttle, M.P., Wolf, L.W., Mayne, P.W., Dyer-Williams, K., and Lafferty, R.H., 2018, Guidance document: Conducting paleoliquefaction studies for earthquake source characterization, U.S. Nuclear Regulatory Agency, NUREG/CR-7238, 185 p.

Tuttle, M.P., Hartleb, R., Wolf, L., and Mayne, P.W., 2019a, Paleoliquefaction studies and the evaluation of seismic hazard, Geosciences, v. 9, n. 7, 61 p. doi:10.3390/geosciences9070311

Tuttle, M.P., Wolf, L.W., Dyer-Williams, K., Mayne, P.W., et al., 2019b, Paleoliquefaction studies in moderate seismicity regions with a history of large earthquakes, U.S. NRC, NUREG/CR-7257, 450 p.

Tuttle, M.P., Dyer-Williams, K., Carter, M.W., Forman, S.L., Tucker, K., Fuentes, Z., Velez, C., and Bauer, L.M., 2021, The liquefaction record of past earthquakes in the Central Virginia seismic zone, Eastern United States, Seismological Research Letters, v. 92, p. 3126-3144 plus electronic supplement. doi: https://doi.org/10.1785/0220200456

Uner, S., 2014, Seismogenic structures in Quaternary lacustrine deposits of Lake Van (eastern Turkey), Geologos, v. 20, p. 79–87. doi:10.2478/logos-2014-0011.

Van de Plassche, O., 1990, Mid-Holocene sea-level change on the Eastern Shore of Virginia, Marine Geology, v. 91, p. 149-154.

Virginia Division of Mineral Resources (DMR), 1993, Geologic map of Virginia, Virginia Division of Mineral Resources, scale 1:500,000.

Witt, A.E., Heller, M., Spears, D., and Hancock, G., 2017, Investigation of brittle structures and soft sediment deformation associated with paleoseismicity along the Lakeside and Little Fork Church faults in the Central Virginia seismic zone: Collaborative research with the Virginia Department of Mines, Minerals and Energy and the United States Geological Survey, Final Technical Report, Prepared for U.S. Geological Survey grant G16AP00139, 20 p.

Wolin, E., Stein, S., Pazzaglia, F., Meltzer, A., Kafka, A., and Berti, C., 2012, Mineral, Virginia, earthquake illustrates seismicity of a passive-aggressive margin, Geophysical Research Letters, v. 39, L02305. doi:10.1029/2011GL050310

Youd, T.L., and Idriss, I.M., 2001, Liquefaction resistance of soils: Summary report from the 1996 NCEER and 1998 NCEER/NSF workshops on evaluation of liquefaction resistance of soils, Journal of Geotechnical and Geoenvironmental Engineering, v. 127, n. 4, p. 297-313.

APPENDIX A PRE-INSTRUMENTAL EARTHQUAKES IN THE CVSZ

Table A-1: Significant Pre-Instrumental Earthquakes in the CVSZ

Catalog[1]	Yr	Mo	Day	Latitude	Longitude	ERH[2]	Mw[3]	E[M][4]	sigM[5]	M Range
SSC	1758	3	23	37.91°	-77.4°	50		4.95	0.371	4.58 -5.32
USGS	1758	3	23	37.91°	-77.4°		4.95		0.371	4.58 -5.32
SSC	1774	2	21	37.2°	-77.4°	45		4.38	0.152	4.23-4.53
USGS	1774	2	21	37.2°	-77.4°		4.43		0.5	3.93-4.93
SSC	1791	1	15	37.5°	-77.5°	40		2.65	0.515	2.14-3.17
USGS	1791	1	15	37.5°	-77.5°		2.68		0.5	2.18-3.18
SSC	1833	8	27	37.7°	-78.0°	38		4.37	0.146	4.22-4.52
USGS	1833	8	27	37.7°	-78.0°		4.38		0.333	4.05-4.71
SSC	1875	12	23	37.6°	-78.5°	34		4.77	0.316	4.45-5.09
USGS	1875	12	23	37.8°	-78.0°		4.77		0.35	4.42 -5.12

[1] SSC - declustered catalog used in CEUS Seismic Source Characterization Project (EPRI et al., 2012); USGS – declustered catalog used in National Seismic Hazard Maps (Mueller, 2019).

[2] Estimated horizontal location uncertainty (km).

[3] Moment magnitude.

[4] Expected value of moment magnitude.

[5] Standard error in the estimated moment magnitude, E[**M**].

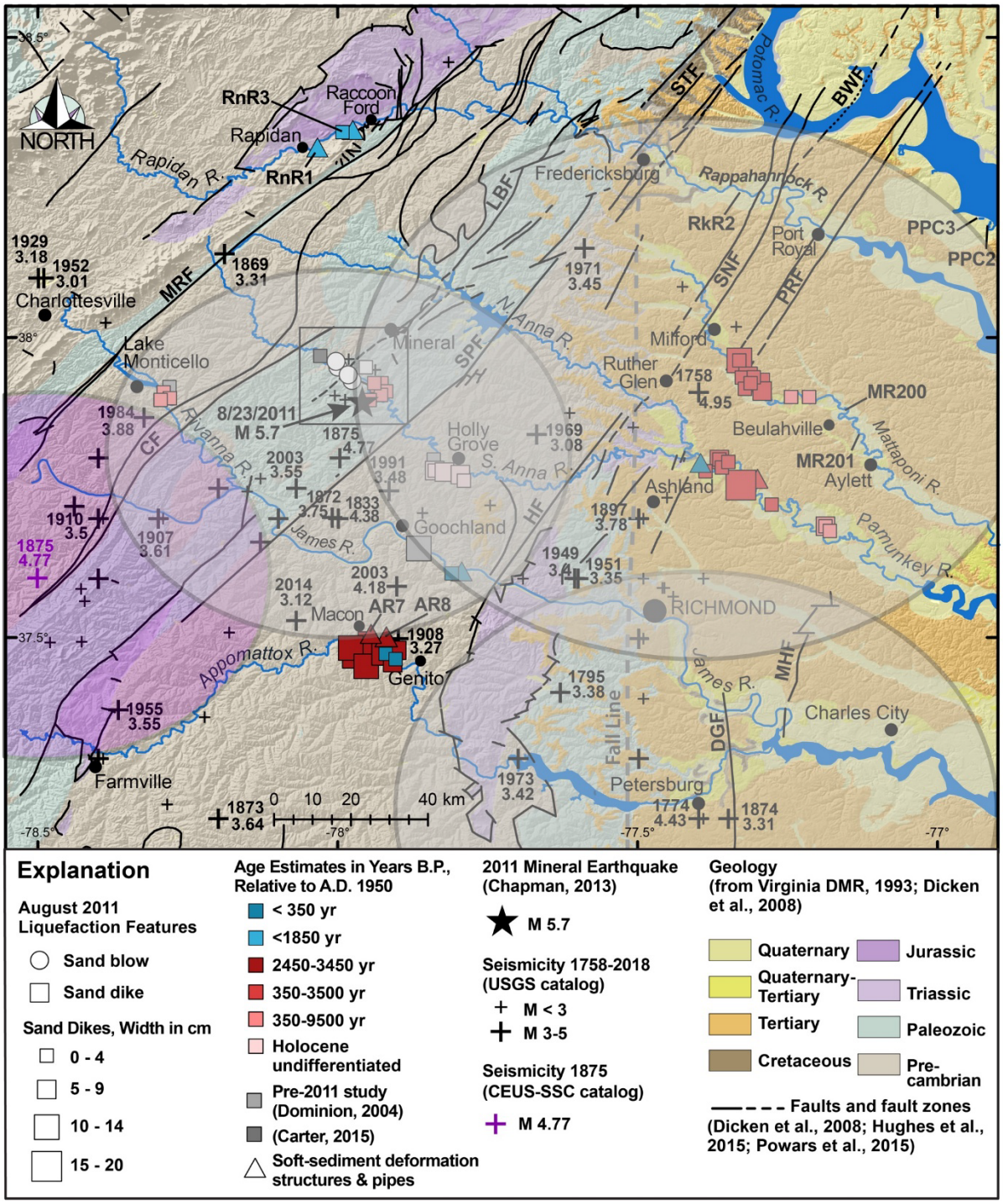

Figure A-1: Map of the CVSZ showing horizontal or epicentral error ellipses for the 1758, 1774, 1833, and 1875 pre-instrumental earthquakes according to the CEUS SSC Project earthquake catalog (EPRI et al., 2012; Table S1). The horizontal error ellipse of the 1875 earthquake is shown for locations according to both the USGS (Mueller, 2019; Rukstales and Petersen, 2019) and CEUS SSC Project earthquake catalogs. Fault zones: CF=Chopawamsic; LBF=Long Branch; MRF=Mountain Run; SPF=Spotsylvania; HF=Hylas; SNF=Skinkers Neck; PRF= Port Royal; DGF=Dutch Gap; and MHF=Malvern Hill.

APPENDIX B GEOLOGIC, GEOTECHNICAL, AND FIELD CONDITIONS

Table B-1: Sedimentary Conditions along Rivers in the CVSZ

River Location	Mapped Surficial Deposits	Exposure From Satellite Imagery
Mattaponi Milford to Rt. 301 bridge	Holocene & Pleistocene alluvium (Qal) [fine to coarse gravelly sand and sandy gravel, silt, and clay; deposited in channel, point-bar, and flood plain environments; up to 15 m thick]; Pleistocene alluvial terrace deposits (Qatu) [fine to coarse gravelly sand, sandy gravel, silt, and clay; surficial deposits of low-lying terraces] †	Heavily forested banks; downed trees in stream bed
Mattaponi Rt. 628 bridge to Rt. 360 bridge	Holocene & Pleistocene alluvium (Qal) [fine to coarse gravelly sand and sandy gravel, silt, and clay; deposited in channel, point-bar, and flood plain environments]; upper Pleistocene, Tabb Formation, Sedgefield Member (Qts) [pebbly to bouldery, clayey sand and fine to medium shelly sand, grading upward to sandy & clayey silt; surficial deposit of river and coast-parallel plains; altitudes 6-9 m]; middle Pleistocene, Shirley Formation (Qsh) [sand, gravel, silt, clay, and peat; surficial deposits of riverine terraces and relict baymouth barriers and bay-floor plains; altitudes 10-14 m]; lower Pleistocene, Charles City Formation (Qcc) [sand, silt, and clay of riverine terraces and coast parallel plains; altitudes 21-24 m; upper Pliocene to lower Miocene, Chesapeake Group (Tc) [fine to coarse sand, silt and clay; deposited in shallow, inner, and middle-shelf waters] ‡	Heavily forested banks; few exposures in river bends
Rappahannock City Dock to Skinkers Neck	Holocene & Pleistocene alluvium (Qal) [fine to coarse gravelly sand and sandy gravel, silt, and clay; deposited in channel, point-bar, and flood plain environments; up to 15 m thick]; upper Pleistocene, Tabb Formation (Qtu) [sand, gravel, silt, and clay underlying low terraces]; middle Pleistocene, Shirley Formation (Qsh) [fine to coarse sand, in part pebbly and bouldery, grades upward to silty fine sand and sandy silt; filling fluvial channels; 10-20 m thick]†	Few exposures in river bends & slump scarps
Rappahannock Skinkers Neck to Port Royal	Holocene & Pleistocene alluvium (Qal) [fine to coarse gravelly sand and sandy gravel, silt, and clay; deposited in channel, point-bar, and flood plain environments; up to 15 m thick]; upper Pleistocene, Tabb Formation, Lynhaven & Poquoson Members (Qtlp) [generally, fine to coarse sand, pebbly and cobbly, grading upward to clayey fine sand & silt; underlying river terraces]; Sedgefield Member (Qts) [pebbly to bouldery, fine to coarse cross-bedded sand, grading upward to sandy & clayey silt; surficial deposit of extensive terraces; up to 15 m thick]; middle Pleistocene, Shirley Formation (Qsh) [fine to coarse sand, in part pebbly and	Few exposures in river bends & slump scarps

River Location	Mapped Surficial Deposits	Exposure From Satellite Imagery
	bouldery, grades upward to silty fine sand & sandy silt; filling fluvial channels; 10-20 m thick] †	
Potomac Mathias Point area	Holocene marsh deposits (Qm) [organic litter, silt, clay, mud, muddy sand, & sand; inter-tidal areas along the margins of estuaries; up to 6 m thick]; upper Pleistocene, Tabb Formation, Sedgefield Member (Qts) [pebbly to boulder, fine to coarse cross-bedded sand, grading upward to sandy & clayey silt; surficial deposit of extensive terraces; up to 15 m thick] †	Along north-east side of Mathias Point, estuary of Upper Macho-doc Creek, & south of Navy Base
Potomac Dahlgren to Popes Creek areas	Holocene marsh deposits (Qm) [organic litter, silt, clay, mud, muddy sand, & sand; inter-tidal areas along the margins of estuaries; up to 5 m thick]; Holocene beach deposits (Qb) [sand, gravel, pebbles, cobbles, boulders; mouths of tributaries; up to 3 m thick]; upper Pleistocene, Tabb Formation, Lynhaven Member (Qtlp) [fine to coarse sand, pebbly and cobbly, grading upward to clayey and silty fine sand & sandy silt]; Sedgefield Member (Qts) [pebbly to bouldery, fine to coarse cross-bedded sand, grading upward to sandy and clayey silt] † *	Along Potomac as well as estuaries of Rosier, and Popes Creeks
Rapidan Bridge in Rapidan to private farm northeast of Racoon Ford	Holocene & Pleistocene alluvium (Qal) [gravel, sand, silt, clay underlying modern flood plains; gravel & sand filling channels at base of fining-upward sequences; 6 m thick]; Pleistocene/Pliocene terrace deposits (QTt) [gravel, sand, silt, clay underlying lowland benches 6-20 m above adjacent modern flood plains; up to 10 m thick] †	River bends & in few slump scarps
Appomattox Farmville area to Rt. 604 bridge crossing near Genito	Holocene and upper Pleistocene alluvium, sand, silt, and clay (this study); probably similar to alluvium along the South Anna River where it crosses the Appalachian Piedmont (Pazzaglia et al., 2015 and 2021; Tuttle et al., 2021)	In Farmville area, few exposures in river bends; farther down-stream, heavily forested banks; few exposures in river bends

‡ From Mixon et al., 1989, Geological map and generalized cross section of the Coastal Plain and adjacent parts of the Piedmont, Virginia, U.S. Geological Survey, Miscellaneous Investigations Series Map I-2033; scale 1:250,000; (map unit) [sediment type].

† From Mixon et al., 2000, Geological map of the Fredericksburg 30' x 60' quadrangle, Virginia and Maryland, U.S. Geological Survey, Geological Investigations Series Map I-2607; scale 1:100,000; (map unit) [sediment type].

* From Newell et al., 2006, Geologic map of the Colonial Beach South 7.5' Virginia quadrangle; U.S. Geological Survey, Open File-2005-1025; scale 1:24,000; (map unit) [sediment type].

Table B-2: Borehole Locations of Geotechnical Data Provided by Virginia Department of Transportation

Site Name (Map ID)	Latitude N (Dec. Degrees)	Longitude W (Dec. Degrees)	Location Description
Rivanna River 1 (1)	37.9186	-78.2977	Rt. 600 bridge near Lake Monticello
So. Anna River 1 (2)	37.9383	-77.9830	Rt. 699 bridge near Yanceyville
So. Anna River 2 (3)	37.7923	-77.8307	Rt. 610 bridge near Holly Grove
James River (4)	37.5768	-77.6793	Rt. 288 bridge west of Richmond
Pamunkey River 1 (5)	37.7889	-77.3699	Rt. 301 bridge near Hanover
Pamunkey River 2 (6)	37.7153	-77.2892	Rt. 615 bridge east of Hanover
Mattaponi River 1 (7)	38.0188	77.3773	Rt. 722 bridge near Milford
Mattaponi River 2 (8)	37.9422	77.3205	Rt. 654 bridge south of Bowling Green
Mattaponi River 3 (9)	37.7869	77.1038	Rt. 360 bridge near Aylett
Rappahannock River 1 (10)	38.2897	77.4497	Rt. 3 bridge near Fredericksburg
Rappahannock River 2 (11)	38.1763	77.1868	Rt. 301 bridge at Port Royal
Potomac River 1 (12)	38.3394	77.0591	Rt. 206 bridge over William Creek near Dahlgren
Potomac River 2 (13)	38.2727	76.9978	Rt. 205 bridge over Tide Mill Stream near Potomac Beach
Rapidan River (14)	38.3590	77.9730	Rt. 522 bridge near Raccoon Ford
Appomattox River 2 (15)	37.4845	77.9654	Rt. 609 bridge south of Macon

Table B-3: Geotechnical Data Gleaned from Borehole Logs

River Location Borehole #	Map ID[1]	Depth (m)	Description of Susceptible Sediment	Blow Count[2]
Rivanna 1	1	7.1	cohesionless sand	5
BH 6		9.4	gray sand with some silt	5
So. Anna 1	2	4.0	yellow-brown silty sand, trace clay with fine to coarse gravel contains mica & thin roots, loose	6
BH 31		5.0	yellow-brown silty sand, trace clay with fine to coarse gravel contains mica and thin roots, very loose	2
		7.0	dark, yellow-brown silty sand, contains mica, very loose	4
So. Anna 2	3	8.0	micaceous, fine, wet sand with organics	6
BH 10		9.0	micaceous, fine, wet sand with organics	11
		11.0	micaceous, fine, wet, fine sand with organics	9
James River	4	4.2	sand, dark brown, wet, loose to dense	6
BH 7		5.3	sand, dark brown, wet, loose to dense	10
		6.3	sand, dark brown, wet, loose to dense	4
Pamunkey 1	5	4.5	gray sand	1
BH 2		6.1	gray sand	5
		7.6	gray gravelly sand	8
		9.1	gray gravelly sand	18
Pamunkey 2	6	6.6	gray sand with black heavy minerals	4
BH 1		7.7	gray sand with black heavy minerals	4
		8.6	gray sand with black heavy minerals	4
Mattaponi 1	7	1.8	sand, gray, fine grained, mottled with brown clay	15
BH 1		3.4	sand, dark gray, fine grained, with clay & shell fragments	11
Mattaponi 2	8	3.1	gray, fine, micaceous silty sand	3
BH 4		4.6	gray, fine, micaceous silty sand	8
Mattaponi 3	9	4.0	gray sand with organics	19
BH 5		5.5		22
Rappahannock 1	10	3.4	brown sand with some organics	5
BH 5		6.4	gray sand	7
Rappahannock 2	11	3.1	tan and gray silty sand	7
BH 40				
Potomac 1	12	15.4	gray sand	9
BH 1				
Potomac 2	13	1.5	white to gray, silty very fine sand	20
BH 006		4.6	white to gray, fine sand, trace of silt	15
Rapidan	14	3.1	light brown silty fine sand with medium gravel	4
BH 5		3.4	towards base	22
Appomattox 2	15	2.4	gray & brown, silty fine to medium sand	9
BH B-1		3.0	gray & brown, silty fine to medium sand	5
		3.4	gray & brown, silty fine to medium sand	4
		3.7	gray & brown, silty fine to medium sand	8
BH R-8		2.4	gray & brown, silty fine sand, contains mica	3
		4.3	gray & brown, silty fine sand, contains mica	2
		5.6	gray & brown, silty fine sand, contains mica	4

[1] Geotechnical site number shown on Figure 1.

[2] Blow count (N) is the total number of blows required to drive a split spoon sampler 0.3 m using standard hammer (63.5 kg) dropping 0.76 m.

APPENDIX C RIVER SURVEYS IN THE CVSZ

Table C-1: Study Sites along Rivers in the CVSZ

Site	Latitude °N Longitude °W	Cutbank Exposure*	Liquefaction Feature*	Weathering of Feature	Constraining Ages Yr B.P. †
Mattaponi River					
MR200	37.8765 77.1492	1 m high – mottled, silt, underlain by interbedded white sand with pebbles & gray silt; pebbles at water level	None	Not applicable	MR200-C1 ≤490
MR201	37.8390 77.1229	6 m high – lower 4 m exposed; sand underlain by bioturbated & mottled silty sand followed by brownish clayey silt with subvertical joints; probe: same as above, then sand 0.5-1+ m BWL	None	Not applicable	MR201-S1 mottled silty sand ≤38470
MR202	37.8309 77.1224	6 m high – lower 2 m exposed; pebbly sand underlain by bio-turbated & mottled silty sand followed by brownish clayey silt with sub-vertical joints; probe: same as above, then sand 0.25+ m BWL	Root casts & joints filled with loose silt and sand	Not applicable	MR201-S1 mottled silty sand ≤38470
Rappahannock River					
RkR1	38.2354 77.3090	1.1 m high – lower 0.6-0.9 m exposed; tan, sand underlain by reddish brown, silt with thin sand layer; probe: silt with interbeds of sand to 1 m, followed by silt to 1.5+ m BWL	None	Not applicable	RkR2-OSL2 reddish silt ≤100
RkR2	38.2435 77.3237	2 m high – mostly exposed; thin, very fine sand at surface; tan, sandy silt under-lain by reddish brown silt; probe: silt with interbeds of sand to 1.5 m BWL	None	Not applicable	RkR2-OSL2 reddish silt ≤100

Site	Latitude °N Longitude °W	Cutbank Exposure*	Liquefaction Feature*	Weathering of Feature	Constraining Ages Yr B.P. †
Potomac-Popes Creek					
PPC1	38.2008 76.9286	3.5 m high – lower 1.5-2.5 m exposed; reddish, fine sandy silt underlain by greenish gray, fine sandy silt, followed by a possible paleosol atop gray, silt with iron-cemented subparallel joints	None	Not applicable	PPC2-C1 clayey silt >43500
PPC2	38.2007 76.9252	3.5 m high – lower 1.5-2.5 m exposed; reddish, fine sandy silt underlain by greenish gray, fine sandy silt, followed by a possible paleo-sol atop gray, silt with iron-cemented subparallel joints	None	Not applicable	PPC2-C1 clayey silt >43500
PPC3	38.1954 76.9095	3 m high – well-exposed; parallel-bedded, pebbly sand underlain by gray & yellowish orange, silt followed by mottled clayey silt	None	Not applicable	PPC2-C1 clayey silt >43500
Rapidan River					
RnR1	38.3186 78.0359	4 m high – lower 1.5 m well exposed; inter-bedded iron-stained sand & silt underlain by gray silt with rock fragments followed by mottled very fine sandy silt; probe: sandy silt to rock at 0.75 m	Soft-sediment deformation – pseudonodules or rounded sandy masses, diapirs and flames	Iron stained	RnR1-C2 close minimum; probably >60; RnR1-C1 <1830; 1830-60; closer in age to RnR1-C2, possibly historical
RnR2	38.3220 78.0342	2 m high – lower 1 m exposed; loose & unweathered, inter-bedded sand & silty sand	None	Not applicable	RnR2-C1 Post 0; modern
RnR3	38.3469 77.9761	3 m high – lower 1.5 m exposed; reddish silt with thin layers of sand overlying bio-turbated & mottled silt & sand;	Sand dike – 1 cm, extends 0.25 m AWL; other sandy domains also in	Dike, gleyed; flames, iron stained	Dike & flames may have formed at same time as SSDs at

Site	Latitude °N Longitude °W	Cutbank Exposure*	Liquefaction Feature*	Weathering of Feature	Constraining Ages Yr B.P. †
		probe: interbedded silt & sand; rock at 0.5 m BWL	bioturba-ted & mottled silt; flames of sand at 0.4 m AWL		RnR1; 1830-60; possibly historical
Appomattox River					
AR5	37.4845 77.9629	3 m high – lower 1 m exposed; yellowish-red, very fine sandy silt, micaceous, with pebbles & cobbles; probe: sandy silt underlain by sand at 1.4+ m	Three dikes – 10 cm, 1 cm, & 0.5 cm wide intruding cracks; extend to 0.6 m AWL or 2.4 m BS	Bioturbated & mottled, iron staining along lower margins of dikes	AR5-OSL1 <27520; AR8-OSL1 >2445; AR8-OSL2 <3450; 3450-2450
AR6	37.4815 77.9531	2.5 m high – lower 2 m exposed; mottled, very fine sandy silt; probe: sandy silt & silt except for sand at 0.33-0.36, 1.30-1.33, & 1.45-1.60 m BWL	One dike – 2 cm wide, branches upward & extends to at least 0.6 m AWL or 1.9 m BS	Bioturbated & mottled, especially upper portion of dikes	AR8-OSL1 >2445; AR8-OSL2 <3450; 3450-2450
AR7	37.4794 77.9474	3 m high – lower 2.5 m exposed; mottled, fining upward silty sand; probe: silty sand underlain by sand at 1.2-1.5+ m BWL	Large, 12 cm wide, dike low in cutbank fed small diapir & two dikes up to 2 cm wide; extends to 0.65 m AWL or 2.35 m BS	Bioturbated & mottled, especially upper portion of dike; iron staining along lower margins	AR7-OSL1 <24525; AR8-OSL1 >2445; AR8-OSL2 <3450; 3450-2450
AR8	37.4783 77.9193	3.8 m high – lower 2.3 m exposed; silty very fine sand underlain by silt loam followed by mottled silt with manganese nodules & mottled silty very fine sand; probe: silty very fine sand to 0.82 m, sand to 0.94 m, followed by silty very fine sand to 1.5 m BWL	Six dikes – 10, 8, 7, 3, 2, & 2 cm wide; extend to 2.04 m AWL or 1.76 m BS, stringers con-tinue to 2.25 m AWL or 1.55 m BS; krotovinas casts injected by sand, become dikes	Older gener-ation dikes - iron stained, mottled, & bioturbated especially along margins; younger generation dikes – unweathered	Older generation: AR8-OSL1 >2445; AR8-OSL2 <3450; 3450-2450; younger generation: probably *hi*storic

* Abbreviations: AWL = above water level; BWL = below water level; BS = below surface, meaning below top of cutbank.

† Yr B.P. before AD 1950 and rounded to the closest decade; > = before and < = after.

APPENDIX D DATING RESULTS

Table D-1: Radiocarbon Dating Performed by Beta Analytic, Inc.

Site-Sample Lab No.[1]	$^{13}C/^{12}C$ Ratio	Conventional ^{14}C Age Yr B.P.[2]	Calibrated ^{14}C Age Yr B.P.[3]	Calibrated Calendar Date[3]	Prob. %	Sample Description[4]
Mattaponi River						
MR200-C1 BA-609013	-25.9	350 ± 30	411-315 490-420	AD 1539-1635 AD 1460-1530	55.4 40	Charred material from silty very fine sand; collected 75 cm BS or 25 cm AWL
MR201-S1 BA-609014	-21.6	32940 ± 230	38474-36679	BC 36525-34730	95.4	Organic sediment from mottled silty sand; collected 10 cm above clayey silt; 4.1 m BS or 1.9 m AWL
Potomac River						
PPC2-C1 BA-609012	-23.9	>43500	NA	NA	NA	Charred material; from brownish, clayey silt; 2.9 m BS or 60 cm AWL
Rapidan River						
RnR1-C1 BA-609015	-24.3	1850 ± 30	1652-1644 1830-1702	AD 298-306 AD 120-248	1.1 94.3	Charred material; from mottled very fine sandy silt below SSD; 3.55 m BS or 45 cm AWL
RnR1-C2 BA-609016	-25.4	170 ± 30	43-Post BP 0 118-60 230-135 290-250	AD 1907- Post AD 1950 AD 1832-1890 AD 1720-1815 AD 1660-1700	19.5 12.5 46.1 17.4	Charred material; from mottled sand layer within inter-bedded sand & silt unit above SSD; 3.08 m BS or 92 cm AWL
RnR2-C1 BA-609017	-24.6	100.88 ± 0.38 pMC	Post 1950	AD 1954-1955	95.4	Charred material; large chunk with rounded corners; from unweathered silty sand; collected 60 cm AWL

[1] BA stands for Beta Analytic, Inc.

[2] Conventional radiocarbon ages in years B.P. or before present (1950) determined by Beta Analytic, Inc. Errors represent 1 standard deviation statistics or 68% probability.

[3] Calibrated age ranges and calendar dates as determined by Beta Analytic, Inc., using the high probability density range method (Bronk Ramsey, 2009) and INTCAL20 (Reimer et al., 2020). Ranges represent 2 standard deviation statistics or 95.4% probability.

[4] Abbreviations: AWL – above water level; BS – below surface of cutbank.

Table D-2: Optically-Stimulated Luminescence Dating Performed by Geoluminescence Dating Research Laboratory

Site-Sample Lab No.	Depth (m)	Cosmic Dose Rate (mGray/yr)[1]	Dose Rate (mGray/yr)	OSL Age (Yr)[2]	OSL Age Yr. B.P.[3]	Sample Description
Rappahannock River						
RkR2-OSL1 BG5421	1.13	0.183 ± 0.018	3.21 ± 0.10	120 ± 10	70-50	From tan, very fine sandy silt
RkR2-OSL2 BG5420	1.63	0.174 ± 0.017	3.15 ± 0.10	150 ± 10	100-80	From reddish brown, silt
Appomattox River						
AR5-OSL1 BG5422	2.91	0.153 ± 0.015	2.16 ± 0.07	25,390 ± 2190	27,520-23,140	From yellowish red, very fine sandy silt, micaceous; 10 cm AWL
AR7-OSL1 BG5419	2.91	0.153 ± 0.015	2.32 ± 0.07	23,600 ± 985	24,525-22555	From reddish, silty medium-fine sand with few pebbles; 10 cm AWL
AR8-OSL1 BG5409	1.45	0.179 ± 0.018	2.37 ± 0.07	2,595 ± 90	2,625-2,445	Near base of upper unit of brownish, silty very fine sand
AR8-OSL2 BG5408	1.59	0.176 ± 0.018	2.45 ± 0.07	3,390 ± 120	3,450-3,210	From reddish brown, very fine sandy silt below silt loam
AR8-OSL3 BG5410	2.39	0.162 ± 0.016	2.15 ± 0.07	2,3055 ± 1010	23,095-21,985	From mottled, silty very fine sand of lower unit

[1] Cosmic dose rate calculated from parameters in Prescott and Hutton (1994) and includes soft components (Liang and Forman, 2019).

[2] Single Aliquot Regeneration age on quartz grains; systematic and random errors calculated in a quadrature at one standard deviation by the Luminescence Dating and Age Calculator (LDAC) at https://www.baylor.edu/geosciences/index.php?id=962356 (Liang and Forman, 2019). Datum year is AD 2010.

[3] Yr. B.P. = year before AD 1950.

APPENDIX E EVALUATIONS OF SCENARIO EARTHQUAKES

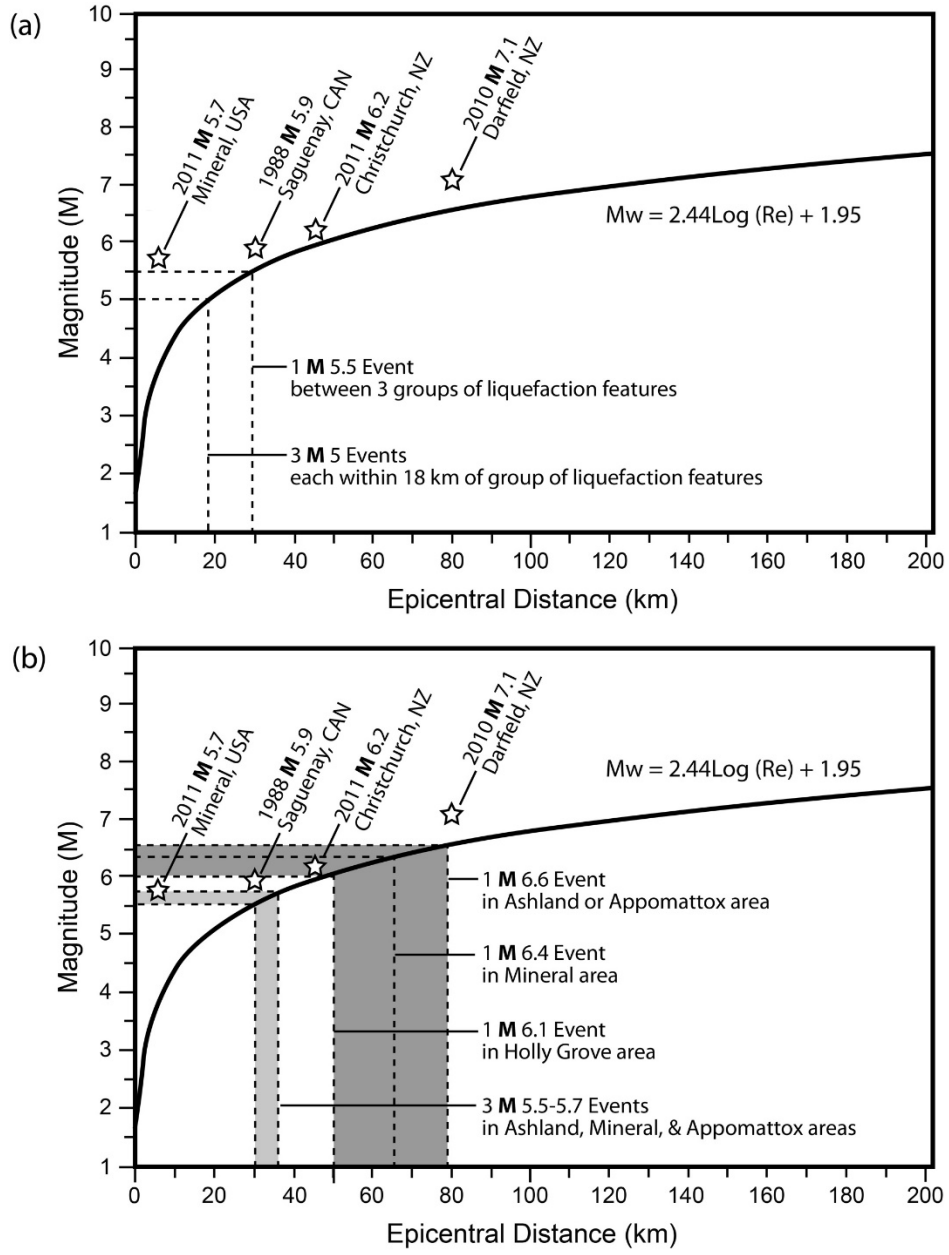

Figure E-1: Relation between moment magnitude (M) and epicentral distance (Re) to farthest liquefaction in very susceptible sediment developed from worldwide data (modified from Castilla and Audemard, 2007). The diagrams show magnitude-distance combinations for (a) pre-instrumental earthquakes that could account for the distribution of historical liquefaction features and (b) paleoearthquakes that could account for prehistorical liquefaction features. Recent earthquakes (white stars) that have induced liquefaction are shown on the diagrams for comparison.

E.1 Cyclic Stress Method for Liquefaction Potential Assessment (LPA)

Scenario earthquakes are evaluated using the cyclic stress method, also known as the simplified procedure, for assessing liquefaction potential (e.g., Seed and Idriss, 1971 and 1982; Youd et al., 2001; Cetin et al., 2004; Idriss and Boulanger, 2004; Green et al., 2005; Tuttle et al., 2019a). In the analysis, peak ground accelerations (PGA) are estimated for scenario earthquakes of moment magnitudes at distances from the possible sources by employing regionally appropriate ground motion prediction equations (GMPEs).

In this study, median GMPEs developed for use in the new generation of seismic hazard maps (Atkinson and Boore, 2011; Atkinson et al., 2012; Atkinson and Assatourians, 2012) are used to calculate peak ground accelerations for the scenario earthquakes. After determining the accelerations, cyclic stress ratios (CSR) generated by scenario earthquakes are calculated using Equation 1,

$$CSR_{7.5} = \frac{\tau_{ave}}{\sigma'_{vo}} = 0.65 \cdot \left(\frac{a_{max}}{g}\right) \cdot \left(\frac{\sigma_{vo}}{\sigma'_{v0}}\right) \cdot r_d \cdot \frac{1}{MSF} \quad (1)$$

where a_{max}=PGA (horizontal component), (a_{max}/g) is PGA divided by the acceleration due to gravity; σ_{vo} and σ'_{v0} are the total and effective vertical overburden stresses, respectively; r_d is a stress reduction coefficient; and MSF is the magnitude scaling factor. The $CSR_{7.5}$ represents the normalized shear stress (τ_{ave}/σ'_{vo}) induced in the soil by the earthquake event (i.e., the seismic demand) and commonly referenced to a benchmark case with moment magnitude, **M** = 7.5.

In the CVSZ region, most of the soil or sediment selected for liquefaction potential analysis fall under site class D, or stiff soils, according to the National Earthquake Hazard Reduction Program (NEHRP) site classification (BSSC, 1997; Dobry et al., 2000). Furthermore, NEHRP recommends site class D be used where soil properties are not known in sufficient detail to make a site class determination. Therefore, site class D is applied to account for soil amplification effects at all sites. PGA (rock) was multiplied by the amplification factor, in this case 1.6, to obtain the a_{max} to be used in Equation 1. To further assess the possible role of soil amplification, site-specific response analysis would be required.

Variations in standard penetration test (SPT) procedure are corrected by adjusting the measured blow count (N_m) using Equation 2:

$$\boldsymbol{N_{1(60)} = C_N\, C_E\, C_B\, C_R\, C_S\, N_m} \quad (2)$$

where $N_{1(60)}$ is normalized blow count corrected for hammer energy (C_E), effective confining stress (C_N), borehole diameter (C_B), rod length (C_R), and sampler configuration (C_S), with N_m being the measured SPT resistance or "blow count" reported in blows/foot (or blows/0.3 m). In this way, the measured N value is standardized to 60% of the potential energy. The correction factors and blow counts are taken from the borehole logs.

Following the computations of the cyclic stress ratio and the adjusted and normalized blow count, the liquefaction potential of representative layers at borehole sites is determined by plotting CSR versus normalized blow count [$(N_1)_{60}$] for **M** 7.5 earthquakes (Seed and Idriss, 1971). If CSR is greater than or equal to cyclic resistance ratio (CRR), the value plots on or above the curve, and the soil is likely to liquefy. Conversely, if CSR is less than CRR, the value plots below the curve, and liquefaction is considered unlikely.

In this study, the approximation to the base curve, the cyclic resistance ratio (CRR), is used, which lends itself to ease of use in spreadsheets. For clean sands, which are tested in boreholes using the SPT, CRR for an **M** 7.5 event proposed by Youd et al. (2001) is given by Equation 3:

$$CRR_{7.5} = \frac{1}{34 - (N_1)_{60-cs}} + \frac{(N_1)_{60-cs}}{135} + \frac{50}{\left[10\,.\,(N_1)_{60-cs} + 45\right]^2} - \frac{1}{200} \quad (3)$$

for $(N_1)_{60\text{-}cs} < 30$; $(N_1)_{60\text{-}cs}$ refers to equivalent clean sand.

The CRR for magnitudes other than 7.5 is calculated by multiplying $CSR_{7.5}$ by the appropriate magnitude scaling factor (MSF), which is given by Equation 4, where M_w represents moment magnitude:

$$MSF = (M_w/7.5)^{-3.3} \quad (4)$$

The following equation is used to calculate the value of the CRR for the evaluation of scenario earthquakes with magnitudes other than 7.5:

$$CRR = CRR_{M7.5} * MSF \quad (5)$$

Once the CSR and the CRR are calculated, the factor of safety against liquefaction (FS_L) is determined using the following equation:

$$FS_L = \frac{CRR}{CSR} \quad (6)$$

The calculated factor of safety (FS) is then used to approximately assess the probability of liquefaction (P_L). As proposed by Juang and Jiang (2000), the probability of liquefaction is calculated using Equation 7:

$$P_L = \frac{1}{1 + (FS\ /\ 1.0)^{3.34}}, \quad (7)$$

where P_L is the probability of liquefaction and *Fs* is the factor of safety. If P_L is greater than or equal to 50%, a layer is likely to liquefy.

Table E-1: Results of LPA for Local Scenario Earthquakes

River Location	Map ID*	Distance† (km)	Results‡ (WT@ 1 m) ‖, #	Results‡ (WT@ 3 m) ‖
1. Scenario earthquake M 5.25				
Mattaponi River 2	8	10	L	N
Rappahannock River 1	10	10	L/N	N
Rappahannock River 2	11	10	N	–
Potomac River 1	12	10	N	N
Rapidan River	14	10	N	–
Appomattox River 2	15	10	L/N	N
2. Scenario earthquake M 5.5				
Mattaponi River 1	7	10	N	N
Mattaponi River 2	8	10	L	L
Mattaponi River 3	9	10	N	N
Rappahannock River 1	10	10	L	L/N
Rappahannock River 2	11	10	L	N
Potomac River 1	12	10	L	L
Potomac River 2	13	10	N	N
Rapidan River	14	10	L	N
Appomattox River 2	15	10	L	L/N
3. Scenario earthquake M 5.75				
Mattaponi River 1	7	10	N	N
Mattaponi River 3	9	10	L	L/N
Rappahannock River 2	11	10	–	L/N
Potomac River 2	13	10	N	N
Rapidan River	14	10	–	L
Appomattox River 2	15	10	–	L

* Geotechnical site number shown on Figure 2-1.

† Distance between scenario earthquake considered and geotechnical site data used in the analysis.

‡ L = Liquefaction likely for 45% - 100% of the layers analyzed; L/N = marginal because liquefaction predicted for 24% - 44% of the layers analyzed; N = liquefaction not likely because liquefaction predicted for less than 24% of the layers analyzed.

‖ WT = water table; depth used in liquefaction potential analysis.

– = Analysis not performed for this scenario earthquake at this water table depth.

Table E-2: Results of LPA for Historical Scenario Earthquakes

River Name	Map ID*	Distance† (km)	Results‡ (WT@1m)‖
1. Scenario earthquake M 4.8			
James River	4	5	N
2. Scenario earthquake M 5.0			
James River	4	5	L/N
James River	4	10	N
Pamunkey River 1	5	10	L/N
3. Scenario earthquake M 5.25			
James River	4	5	L
James River	4	10	L/N
James River	4	15	N
Pamunkey River 1	5	10	L
Pamunkey River 1	5	15	L/N
Appomattox River 2	15	10	L
Appomattox River 2	15	15	N
4. Scenario earthquake M 5.5			
James River	4	10	L
James River	4	15	L/N
James River	4	20	N
Pamunkey River 1	5	15	L
Pamunkey River 1	5	20	N
Appomattox River 2	15	15	L/N
Appomattox River 2	15	30	N
5. Scenario earthquake M 5.75			
James River	4	20	L/N
James River	4	30	N
Pamunkey River 1	5	20	L
Pamunkey River 1	5	30	L/N
Mattaponi River 3	9	30	N
Rapidan River	14	20	N
Appomattox River 2	15	15	L
Appomattox River 2	15	20	L
Appomattox River 2	15	30	N
5. Scenario earthquake M 6			
James River	4	30	L/N
Pamunkey River 1	5	30	L
Rapidan River	14	20	L
Appomattox River 2	15	30	L/N

See footnotes below Table E-1.

Table E-3: Results of LPA for Mineral Scenario Earthquakes

River Location	Map ID*	Distance† (km)	Results‡ (WT@ 1 m)‖, #	Results‡ (WT@ 3 m)‖
1. Scenario earthquake M 5.25				
South Anna 1	2	10	L	N
2. Scenario earthquake M 5.5				
South Anna 1	2	10	–	L
Pamunkey 1	5	55	–	N
3. Scenario earthquake M 5.75				
South Anna 2	3	20	L	N
4. Scenario earthquake M 6.0				
South Anna 2	3	20	–	L
Rivanna 1	1	30	L	N
Appomattox 2	15	47	N	–
Rapidan	14	50	N	–
5. Scenario earthquake M 6.25				
Rivanna 1	1	30	–	L
Appomattox 2	15	47	N	–
Rapidan	14	50	N	–
Pamunkey 1	5	55	L/N	N
Pamunkey 2	6	65	N	N
6. Scenario earthquake M 6.5				
Appomattox 2	15	47	L	L/N
Rapidan	14	50	L/N	N
Pamunkey 1	5	55	L	L/N
Mattaponi 2	8	58	N	N
Rappahannock 1	11	63	N	–
Pamunkey 2	6	65	L	N
7. Scenario earthquake M 6.75				
Appomattox 2	15	47	–	L
Rapidan	14	50	L	L
Pamunkey 1	5	55	–	L
Mattaponi 2	8	58	L	N
Rappahannock 1	11	63	L	N
Pamunkey 2	6	65	–	L
Mattaponi 3	9	78	N	N
8. Scenario earthquake M 7.0				
Mattaponi 2	8	58	–	L
Rappahannock 1	11	63	–	L
Mattaponi 3	9	78	N	N
Potomac 1	12	94	N	N

See footnotes below Table E-1.

Table E-4: Results of LPA for Holly Grove Area Scenario Earthquakes

River Location	Map ID*	Distance† (km)	Results‡ (WT@ 1 m) ‖, #	Results‡ (WT@ 3 m) ‖
1. Scenario earthquake M 6.0				
South Anna River 1	2	15	L	L
Appomattox River 2	15	36	N	–
Rivanna River 1	1	43	N	–
Pamunkey River 2	6	48	N	–
2. Scenario earthquake M 6.25				
South Anna River 1	2	15	L	L
Appomattox River 2	15	36	L	N
Rivanna River 1	1	43	L	N
Pamunkey River 2	6	48	L	N
Mattaponi River 2	8	48	N	N
3. Scenario earthquake M 6.5				
Appomattox River 2	15	36	–	L
Rivanna River 1	1	43	–	L
Pamunkey River 2	6	48	–	L
Mattaponi River 2	8	48	L	N
Mattaponi River 3	9	64	N	–
Rappahannock River 1	11	64	N	–
Rapidan River	14	64	N	–
Potomac 1	12	91	N	–
4. Scenario earthquake M 6.75				
Mattaponi River 2	8	48	L	L
Mattaponi River 3	9	64	N	–
Rappahannock River 1	11	64	L	L/N
Rapidan River	14	64	L/N	N
Potomac 1	12	91	N	–
5. Scenario earthquake M 7.0				
Mattaponi River 3	9	64	N	–
Rapidan River 1	14	64	L	L
Potomac 1	12	91	L	N

See footnotes below Table E-1.

Table E-5: Results of LPA for Ashland Area Scenario Earthquakes

River Location	Map ID*	Distance† (km)	Results‡ (WT@ 1 m)‖, #	Results‡ (WT@ 3 m)‖
1. Scenario earthquake M 5.25				
Pamunkey 1	5	10	L	L/N
Pamunkey 2	6	16	N	N
2. Scenario earthquake M 5.5				
Pamunkey 1	5	10	–	L
Pamunkey 2	6	16	L	L
Mattaponi 2	8	18	L	N
3. Scenario earthquake M 5.75				
Mattaponi 2	8	18	L	N
4. Scenario earthquake M 6.0				
Mattaponi 2	8	18	–	L
Mattaponi 3	9	29	N	–
South Anna 2	3	35	N	N
South Anna 1	2	45	N	N
5. Scenario earthquake M 6.25				
Mattaponi 3	9	29	N	–
South Anna 2	3	35	L	L
South Anna 1	2	45	L	N
Rappahannock 1	11	54	N	–
Appomattox 2	15	58	N	–
6. Scenario earthquake M 6.5				
Mattaponi 3	9	29	L	N
South Anna 1	2	45	–	L
Rappahannock 1	11	54	L/N	N
Appomattox 2	15	58	L/N	N
Potomac 1	12	68	N	–
Rivanna 1	1	78	N	N
7. Scenario earthquake M 6.75				
Mattaponi 3	9	29	–	L/N
Rappahannock 1	11	54	L	L/N
Appomattox 2	15	58	L	L/N
Potomac 1	12	68	N	–
Rivanna 1	1	78	L	L
Rapidan	14	78	N	N
8. Scenario earthquake M 7.0				
Appomattox 2	15	58	–	L
Potomac 1	12	68	L	L
Rapidan	14	78	L	N

See footnotes below Table E-1.